Chapter 8

Physics of Top Quarks

8.1 Selection of $t\bar{t}$ events and measurement of the cross sections

8.1.1 Introduction

The goal of top physics at the LHC is to characterise the properties of this heaviest fermion of the Standard Model by measuring observables in its production and decay exploiting all possible decay channels. Important examples are the production cross section and the mass and spin properties of the top quark.

Most of the top quarks at the LHC will be produced as $t\bar{t}$ pairs. The $t\bar{t}$ production cross section is estimated to be $830\,\text{pb}$ [277] at NLO and the dominant production mechanisms are gluon-gluon fusion ($\approx 90\%$) and quark-anti-quark annihilation ($\approx 10\%$). Within the Standard Model the top quark decays almost exclusively to a W boson and a b quark. The decays of the $t\bar{t}$ system are then classified according to the decays of the W^+W^- system as dileptonic, semi-leptonic or fully hadronic. The W can decay into leptons, $e^-\bar{\nu}_e, \mu^-\bar{\nu}_\mu, \tau^-\bar{\nu}_\tau$, or into quarks, $u\bar{d}', c\bar{s}'$, where the charge conjugate is implicit. Neglecting QCD corrections, branching fractions of 9/81 (11.1%) for the dileptonic, 36/81 (44.4%) for the semi-leptonic and 36/81 (44.4%) for the fully hadronic decay channel are obtained.

For our studies we use PYTHIA for the simulation of signal and background events. As it includes spin correlation in $t\bar{t}$ production also samples generated with TOPREX are used for signal events.

8.1.2 Dileptonic channel

8.1.2.1 Event selection for 1 fb^{-1}

The very clean signature of this channel combined with a high signal-to-background ratio makes it possible to select $t\bar{t}$-events with simple kinematic cuts. The selection is therefore suitable for the expected early performance of the CMS detector and will allow to establish the signal as well as to measure the top mass at an early stage of the experiment.

For an integrated luminosity of $1\,\text{fb}^{-1}$ about 54000 signal events are expected according to the leading-order estimate of PYTHIA. The main backgrounds with a final state mimicking the signal are Z, WW, WZ and ZZ production accompanied by jets. Furthermore, events from semi-leptonic and fully-hadronic top-quark pair production with misidentified leptons and leptons from b-quark jets eventually constitute the dominating background. Here, dilepton events with W bosons decaying into τ-leptons are considered signal events if the τ lepton

decays leptonically. Details of the analysis can be found in Reference [278].

Events are required to pass the Level-1 and High Level Trigger, in particular the single and dilepton subtriggers. In addition to trigger criteria, events must contain at least two jets and two oppositely charged leptons. Electrons are identified using an electron likelihood method combining various electromagnetic shower variables and track-to-supercluster-matching criteria. After this pre-selection about 15000 signal events are left in a $1\,\mathrm{fb}^{-1}$ data set with a signal over background ratio of $S/B = 1/10$. The most important background at this stage consists of $Z + \mathrm{jets}$ production with an accepted cross section of about 120 pb and a similar final state.

Isolation criteria reduce the contribution from misidentified leptons and leptons from b-jets. For a lepton candidate no other track or calorimeter hits amounting to 10% or more of the lepton p_T are allowed in a cone of $\Delta R < 0.2$. Two charged leptons are then chosen with a discriminant based on the likelihood ratio in case of an electron, the energy deposited in a cone of $\Delta R = 0.2$ around the lepton axis and the p_T of the lepton.

Both b-jets are selected with a discriminator based on the jet p_T, the invariant mass of tracks inside the jet and the output of the combined b-tagging algorithm [156]. Using this scheme the correct jets and leptons of the signal are selected for more than 90% of the events, if they could be reconstructed. It has been shown in reference [156] that, during the *first data taking phases* of the LHC, the degradation in b-tagging performance is still acceptable. This implies that the b-tagging results presented here remain essentially correct.

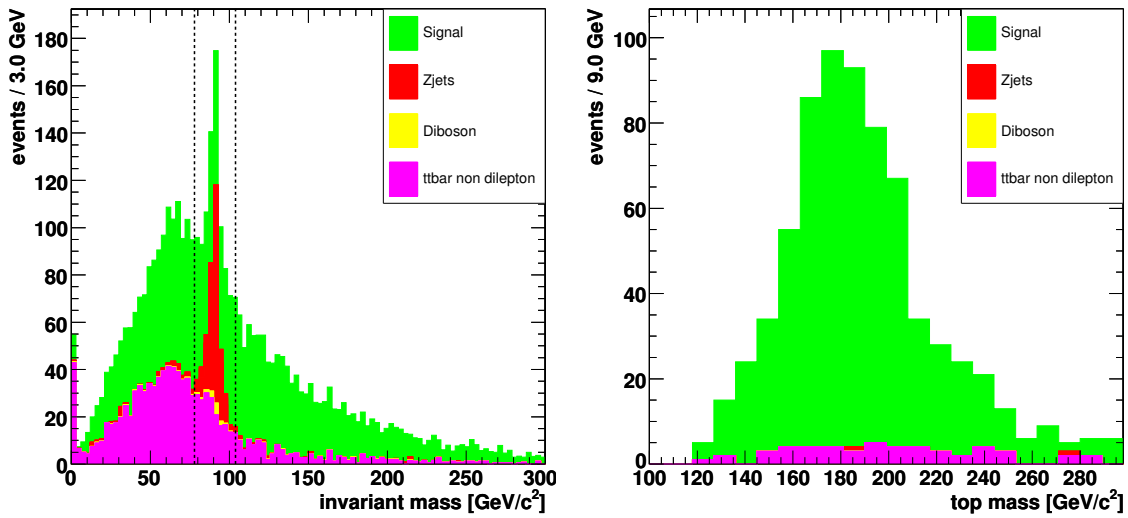

Figure 8.1: Left: Invariant mass of the two lepton candidates indicating the cut window to remove $Z + \mathrm{jets}$ events. Right: Most likely top mass after selection for $1\,\mathrm{fb}^{-1}$.

Figure 8.1 shows the invariant mass of the two lepton candidates. The Z mass peak of the invariant mass distribution of two same type leptons is used to remove the contamination due to $Z + \mathrm{jets}$ events. As a further improvement a cut on the b-tag discriminator is applied to the two selected jets.

The non-dilepton $t\bar{t}$ events usually contain more jets with a p_T greater than $30\,\mathrm{GeV/c}$ but do not contain two high p_T leptons. The second lepton candidate is considerably softer than the corresponding lepton from the signal decay channel. So a cut on the lower transverse

momentum lepton is imposed with $p_{\mathrm{T}} > 20\,\mathrm{GeV/c}$. The two neutrinos in the decay of the W bosons lead to significant missing transverse energy $E_{\mathrm{T}}^{\mathrm{miss}}$ whereas the decay of Z bosons into electrons or muons does not generate $E_{\mathrm{T}}^{\mathrm{miss}}$. The cut $E_{\mathrm{T}}^{\mathrm{miss}} > 40\,\mathrm{GeV}$ further improves the signal to background ratio. At this stage about 1800 signal events are left with a signal over background ratio of $S/B = 7.3/1$.

The kinematics of the $t\bar{t}$ dilepton events yield an underconstrained equation system due to the two undetected neutrinos in the final state. However if all other kinematic quantities have been measured it is possible to make a fit imposing m_W and assuming a top mass parameter in the range of 100 to $300\,\mathrm{GeV/c^2}$. A weight can then be assigned to the different solutions obtained [278]. Figure 8.1 shows the distribution of the most likely top mass for signal and background events in the range $100\,\mathrm{GeV/c^2} < m_t < 300\,\mathrm{GeV/c^2}$.

The event topology of most of the background events passing the previous cuts does not satisfy the dilepton kinematical constraints. Therefore considering only candidates which give a mass estimate in the range of 100 to $300\,\mathrm{GeV/c^2}$ further reduces the background and raises the signal over background ratio to about $S : B = 12 : 1$. The remaining background essentially contains only non-dilepton $t\bar{t}$ events. In a dataset equivalent to $1\,\mathrm{fb}^{-1}$, 657 signal events are selected with an overall efficiency of 1.2%.

We conclude that a measurement of the $t\bar{t}$ cross section and the top mass (see Section 8.2.1) in the dileptonic channel will be possible already with a modest amount of luminosity [278].

8.1.2.2 Event selection for higher luminosities

The trigger is based on the presence of one muon or electron which covers with high efficiency all the possible final states in this channel. The selection of events in this channel then requires after trigger selection the presence of just two oppositely charged leptons with $E_{\mathrm{T}} > 20\,\mathrm{GeV}$ within pseudorapidity ranges of ± 2.4 and ± 2.5 for muons and electrons respectively. Details are available in [278].

The reconstruction efficiency is good for both for muons and electrons. More than 97% of the generated muons are correctly reconstructed in the considered range, as well as 90% of the electrons, with p_{T} above $20\,\mathrm{GeV/c}$ [278]. An electron is considered isolated if the total uncorrected E_{T} of the jets within a cone $\Delta R \leq 0.3$, minus the lepton E_{T}, is less than 30% of the lepton E_{T}. In a similar way a muon is considered isolated, if the sum of the p_{T} of all the tracks present in a cone of $\Delta R \leq 0.3$ minus p_{T} of the muon is less than $2\,\mathrm{GeV/c}$. Candidate events must have $E_{\mathrm{T}}^{\mathrm{miss}} > 40\,\mathrm{GeV}$. The analysis requires at least two jets with uncorrected $E_{\mathrm{T}} > 20\,\mathrm{GeV}$ detected within $|\eta| < 2.5$, where a jet is defined as a fixed-cone cluster with a cone size of $R = 0.5$. Jets produced by electrons are discarded before applying the previous selection by removing those which have an electromagnetic supercluster within $\Delta R = 0.2$ with a ratio between the electromagnetic energy of that supercluster and the uncorrected jet energy above 0.75.

b-tagging techniques based on the explicit reconstruction of a secondary vertex in a jet [156] are used to further suppress backgrounds in which no jets from b-quarks are present. The dominant backgrounds to dilepton $t\bar{t}$ events are those which have real leptons, real $E_{\mathrm{T}}^{\mathrm{miss}}$ and jets originating from initial or final state radiation, arising mainly from dibosons (WW, WZ, and ZZ) + jets production, and also from top quark decays, either from the semi-leptonic channel or from tau decays producing leptons. This kind of backgrounds are expected to be determined using MC simulation. Instrumental backgrounds, are characterised in general

Table 8.1: Cumulative effect of the different selection criteria applied to the simulated $t\bar{t}$ dilepton sample (electrons and muons) and simulated backgrounds. The column denoted as τ corresponds to $t\bar{t}$ dilepton sample in which at least one W decays into a τ lepton. The numbers correspond to LO accepted cross sections in pb.

	Signal	τ	WW	WZ	ZZ	$Z+\text{jets}$	other $t\bar{t}$
Before selection	24.3	30.4	7.74	0.89	0.11	3912	438
Level-1 + HLT	19.4	15.1	4.4	0.37	0.07	657	92
2 jets $E_{\mathrm{T}} > 20\,\mathrm{GeV}$	11.5	9.8	0.6	0.012	0.006	23.9	73.1
$E_{\mathrm{T}}^{\mathrm{miss}} > 40\,\mathrm{GeV}$	9.6	8.1	0.5	0.01	0.003	5.8	53.6
Two opp. charged leptons	3.2	0.42	0.04	0.001	0.001	1.17	0.12
b-tag of two highest E_{T} jets	1.12	0.15	0.002	$\sim 10^{-4}$	$\sim 10^{-5}$	< 0.01	0.05

by their large cross sections but not having real $E_{\mathrm{T}}^{\mathrm{miss}}$, among them are: $Z+\text{jets}$, Drell-Yan ($Z/\gamma^{\star} \rightarrow \ell^{+}\ell^{-}$) production, "fake" leptons in $W \rightarrow \ell\nu + \text{jet}$ events where a jet is falsely reconstructed as a lepton candidate. In principle it is harder to estimate their contribution to the final sample using MC simulation.

After this selection an efficiency close to 5% is obtained, with a very high rejection of all the backgrounds considered at the level of $10^{-3} : 1$ or better, as shown in Table 8.1. A S/B value of 5.5 is obtained, the main background being the one arising from the dilepton channel itself in which at least one of the W decays into $\tau\nu_{\tau}$ and with a subsequent leptonic tau decay.

Different sources of systematic uncertainties have been identified that affect event selection and background determination and thus the cross section measurement. Detailed studies [278] of these sources have been done based mainly on the results of the studies performed in [7] and [200]. Among the most important experimental sources are uncertainties on the jet energy scale and the b-tag efficiency. The impact of theoretical and phenomenological uncertainties such as those on hadron fragmentation and PDF have been studied using samples generated with different PYTHIA parameters and simulated and reconstructed with the CMS fast simulation and reconstruction program. The uncertainty in the cross section coming from the luminosity estimation was taken as 3% as expected for $10\,\mathrm{fb}^{-1}$ integrated luminosity. As the non-$t\bar{t}$ background is small it does not contribute significantly to the uncertainty. The results are summarised in Table 8.2 and lead to an estimated total error on the $t\bar{t}$ cross section measured in the dileptonic channel using electrons and muons of $\Delta\sigma_{t\bar{t}}/\sigma_{t\bar{t}} = 11\%\ (syst)\ \pm 0.9\%\ (stat)\ \pm 3\%\ (luminosity)$.

Table 8.2: Uncertainties in the $t\bar{t}$ dilepton cross section determination for $10\,\mathrm{fb}^{-1}$.

Effect	$\Delta\sigma_{t\bar{t}\ dil\ e/\mu}/\sigma_{t\bar{t}\ dil\ e/\mu}$
Jet Energy Scale	3.6%
b-tag efficiency	3.8%
Lepton reconstruction	1.6%
$E_{\mathrm{T}}^{\mathrm{miss}}$	1.1%
ISR and FSR	2.5%
Pile-Up	3.6%
Underlying Event	4.1%
Heavy quark fragmentation	5.1%
PDF uncertainties	5.2%
Statistical uncertainty	0.9%
Integrated luminosity	3%

8.1.2.3 Top decays to tau leptons

In this section studies performed to select events with τ leptons in the final state are presented. We consider here dileptonic $t\bar{t}$ decays with one tau lepton decaying into hadrons in the final state $t\bar{t} \rightarrow b\bar{b}\tau\nu_\tau\ell\nu_\ell$, $(\ell = \mathrm{e}, \mu)$. The measurement of the ratio $BR(t\bar{t} \rightarrow \ell\tau + X)/BR(t\bar{t} \rightarrow \ell\ell + X)$ will allow to set new limits on the presence of non-standard physics in top decays. Furthermore, this channel is a source of background for Supersymmetry and Higgs searches, as well as for the other dileptonic top channels.

Table 8.3: Cumulative effect of the different selection criteria applied to the simulated $t\bar{t}$ sample. Numbers correspond to LO accepted cross sections.

Cut	Efficiency times cross sections (pb)			
	$t\bar{t}$ (signal)	$t\bar{t}$ (other dilepton)	$t\bar{t}$ (semi-leptonic)	$t\bar{t}$ (hadronic)
Before selection	15.62	38.94	218.88	218.88
Trigger	8.61	25.40	85.90	2.08
2 jets	6.97	18.90	80.08	2.04
≥ 1 Iso lepton	4.27	13.11	34.93	0.11
$E_{\mathrm{T}}^{\mathrm{miss}} \geq 40\,\mathrm{GeV}$	3.58	10.89	26.41	0.05
1 lepton	3.48	6.73	25.24	0.04
τ cand. with opp. Q	0.75	0.20	0.75	0.001
b-tagging	0.29	0.07	0.30	0.0005

Tau candidates are selected and identified following the method of the MSSM Higgs and HLT analyses [279], adapting the different selection criteria to the momentum range in which tau candidates are expected to be produced in top decays [278] . The hadronic tau identification efficiency obtained in the dilepton samples is about 30% using this method as can be seen in Figure 8.2.

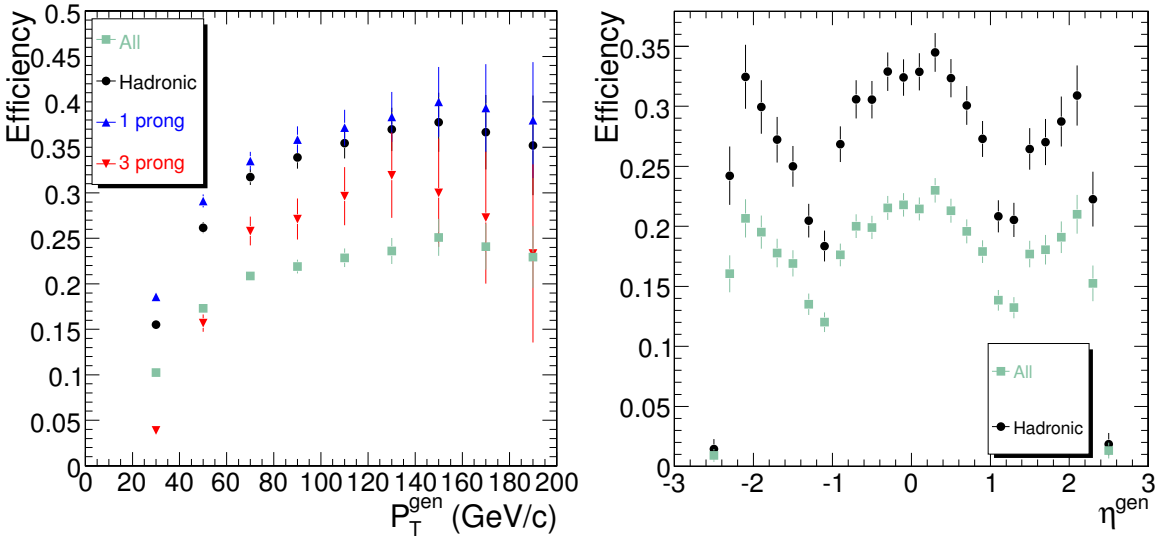

Figure 8.2: Reconstruction efficiency of tau candidates as a function of p_{T} and η. Errors are statistical only.

Event selection proceeds in a similar way as in section 8.1.2.2 but only one isolated lepton (electron or muon) is allowed. One isolated tau candidate separated from the isolated lepton

has to be present, and the isolated lepton and the tau candidate must have opposite charges. The effect of these selections are described in detail for the $t\bar{t}$ sample in Table 8.3. b-tag for the two accompanying jets is also required. An efficiency close to 2% is obtained, with a very high rejection of all the backgrounds considered. A S/B value close to 1 is obtained, the main background being the one arising from the $t\bar{t}$ semi-leptonic channel. The majority of the systematic uncertainties are described in section 8.1.2.2. There is another systematic uncertainty intrinsic to this analysis due to the τ reconstruction and identification. Based on preliminary studies, we assigned a 12% uncertainty to the τ reconstruction and identification. Statistical uncertainty in the cross section determination is about 1.3% for an integrated luminosity of 10 fb^{-1}. Then the relative uncertainty in the estimation of the cross section is given by $\Delta\sigma_{t\bar{t}\ dil\ \tau,e\mu}/\sigma_{t\bar{t}\ dil\ \tau,e\mu} = 16\%\ (syst)\ \pm 1.3\%\ (stat)\ \pm 3\%\ (luminosity)$.

8.1.3 Semi-leptonic channel

The semi-leptonic $t\bar{t}$ decay has a final state topology of four hadronic jets of which two originate from a b-quark, an isolated lepton and missing transverse momentum. In this section we consider the measurement of the cross section of the semi-leptonic $t\bar{t}$ production where the lepton is a muon [280].

Both the Level-1 and the High-Level Trigger selection criteria are applied on the simulated events, resulting in the efficiencies shown in Table 8.4. The single-muon trigger stream was used. The jets are reconstructed from the combined electromagnetic and hadronic calorimeter energy deposits and clustered with the Iterative Cone algorithm using an opening angle of $\Delta R = 0.5$. A transverse energy threshold of 0.5 GeV is applied on the input objects before clustering. Optimisation of the parameter settings of the clustering algorithms are considered in [281]. Only the jets in the vicinity of the primary vertex are considered in the analyses, rejecting in general those jets with a small transverse momentum. The energy scale of the reconstructed jets is calibrated using the methods described in [282]. Among the list of muon candidates identified flavour, the muon originating directly from the W boson decay is selected following the procedure described in [283]. The transverse momentum components of the unobserved neutrino are estimated via the missing transverse momentum which balances the vectorial sum of the energy deposits in the calorimeter above the transverse energy threshold mentioned.

Table 8.4: Overview of the selection criteria applied. The expected S/B values take into account the respective Leading-Order cross-sections of the processes.

	Semi-lept. $t\bar{t}$	Other $t\bar{t}$	W+4j	Wbb+2j	Wbb+3j	S/B
Before selection	365k	1962k	82.5k	109.5k	22.5k	5.9
L1+HLT Trigger	62.2%	5.30%	24.1%	8.35%	8.29%	7.8
Four jets $E_T > 30$ GeV	25.4%	1.01%	4.1%	1.48%	3.37%	9.9
$p_{\mathrm{T}}^{lepton} > 20$ GeV/c	24.8%	0.97%	3.9%	1.41%	3.14%	10.3
b-tag criteria	6.5%	0.24%	0.064%	0.52%	0.79%	25.4
Kinematic fit	6.3%	0.23%	0.059%	0.48%	0.72%	26.7
Selected cross section (pb)	5.21	1.10	0.10	0.08	0.05	26.7
Scaled $\mathcal{L} = 1$ fb^{-1}	5211	1084	104	82	50	26.7

The event selection consists of a series of sequential cuts on kinematic or topological variables. The event is required to have at least four jets after applying the primary vertex constraint with a calibrated transverse energy, E_{T}, exceeding 30 GeV and within a pseudo-

rapidity in the range of the tracker, $|\eta| < 2.4$. If more than four jets match this criterion, the four leading jets are selected as those with the highest E_{T}. Of these four jets, two have to be b-tagged according to the method applying a combined b-tag variable described in [280, 284, 285]. The selected lepton is required to be within the tracker acceptance and to have a transverse momentum larger than $20\,\mathrm{GeV/c}$.

After classifying two of the four reconstructed jets as b-quark and the other two as light quark jets, only two jet combinations remain to reconstruct the hadronically-decaying top. A kinematic fit [166] was applied on the reconstructed event for both jet combinations forcing the reconstructed W boson mass to its precisely known value. Before applying the kinematic fit the energy scale of the light quark jets is corrected for an overall bias in the reconstructed W boson mass. Following the method described in [286] after the event selection mentioned above, an inclusive jet energy scale correction of -9.7% was obtained and applied to light quark jet candidates. The event is finally selected if the fit converged for at least one of the combinations.

The selection efficiency for the signal events is estimated to be 6.28 ± 0.04 %. The fraction of $t\bar{t}$ signal events in the selected sample of inclusive $t\bar{t}$ decays is estimated to be 82.8 ± 0.2 %. The signal-to-background ratio after the event selection is 26.7, where all $t\bar{t}$ decay channels are considered as signal. Hence the systematic effect of the background contribution is minor. It is shown in [280] that after the event selection topological observables will not help much in differentiating between signal and background. The cross section is therefore estimated from counting events. The statistical uncertainty on the estimated cross section is 1.2%, 0.6% and 0.4% for integrated luminosities of $1\,\mathrm{fb}^{-1}$, $5\,\mathrm{fb}^{-1}$ and $10\,\mathrm{fb}^{-1}$, respectively.

Systematic effects are introduced only on the signal events, changing the efficiency of the event selection. Similar effects on the background samples should be a second order effect on the inferred cross section. For the theoretical or phenomenological uncertainties the prescription of [200] was used as described in [280]. The list of systematic uncertainties is shown in Table 8.5. The dominant systematic effects are b-tagging, and in the early stage the uncertainty on the integrated luminosity. For an extended discussion on the studied systematic effects we refer to [280]. As a consequence of the kinematic fit, the uncertainty on both the light- and heavy-quark jet energy scale results in a limited systematic uncertainty, of about 1.6%.

The total relative systematic uncertainty on the cross section is 10.5% which can be compared to a relative statistical uncertainty of 0.6% at $5\,\mathrm{fb}^{-1}$. The total uncertainty of 10.5% scales with the integrated luminosity as shown in Figure 8.3. In this plot it is assumed that the uncertainty on the determination of the integrated luminosity scale as the inverse square root of the integrated luminosity. At an integrated luminosity of about $5\,\mathrm{fb}^{-1}$ the total uncertainty is dominated by the uncertainty on the b-tagging performance. For the uncertainty on the b-tagging efficiency a conservative 5% is taken according to [285] although the Tevatron experience shows that a value of 2% can be reached [287, 288].

8.1.4 Fully hadronic channel

The fully hadronic final state, characterised by a six-jets topology $t\bar{t} \to WWb\bar{b} \to qqqqb\bar{b}$, has the largest branching fraction (46%), and kinematics that can be fully reconstructed. However, this channel is affected by a large background from QCD multi-jet production, which makes the isolation of the signal rather challenging, and internal jet-parton permutation uncertainties. Improvements in the signal-to-background ratio are possible by requiring the

Table 8.5: Overview of the systematic uncertainties on the cross section.

	$\Delta\hat{\sigma}_{t\bar{t}(\mu)}/\hat{\sigma}_{t\bar{t}(\mu)}$		
	$1\,\text{fb}^{-1}$	$5\,\text{fb}^{-1}$	$10\,\text{fb}^{-1}$
Simulation samples (ϵ_{sim})		0.6%	
Simulation samples (F_{sim})		0.2%	
Pile-Up (30% On-Off)		3.2%	
Underlying Event		0.8%	
Jet Energy Scale (light quarks) (2%)		1.6%	
Jet Energy Scale (heavy quarks) (2%)		1.6%	
Radiation (Λ_{QCD}, Q_0^2)		2.6%	
Fragmentation (Lund b, σ_q)		1.0%	
b-tagging (5%)		7.0%	
Parton Density Functions		3.4%	
Background level		0.9%	
Integrated luminosity	10%	5%	3%
Statistical Uncertainty	1.2%	0.6%	0.4%
Total Systematic Uncertainty	13.6%	10.5%	9.7%
Total Uncertainty	13.7%	10.5%	9.7%

presence of b-quark jets and by selecting central and very high-energy kinematic configurations which are expected for jets arising from the decay of a massive object like the top quark. A specific multi-jet trigger which uses b-tagging information has been devised for this analysis and an optimised selection has been applied. The analysis is described in detail in [278].

The signal sample consists of 500000 inclusive $t\bar{t}$ events, from which a sub-sample of 230000 fully hadronic $t\bar{t}$ events is extracted. The background consists of 1.5 million multi-jet events (QCD) generated with $50 < \hat{p_{\text{T}}} < 470\,\text{GeV/c}$, where the $\hat{p_{\text{T}}}$ symbol indicates the transverse momentum of the most energetic parton of the hard scattering before the final-state radiation processes.

8.1.4.1 Trigger pre-selection and event selection

The trigger pre-selection uses the inclusive jet trigger envisaged in [75] and a special inclusive b-jet trigger [289]. The inclusive b-jet trigger combines in the first stage the b-tagging requirement with an inclusive jet trigger which applies tuned E_{T} thresholds of 350 GeV for single jets, 150 GeV for 3-jet and 55 GeV for 4-jet topologies; then a b-tagging based on pixel and regional track and vertex reconstruction is performed on the two most energetic jets. The trigger requires either multiple jets in the event or a b-tagged jet among the two highest-E_{T} jets. After the trigger pre-selection the QCD rate is reduced to 23 Hz, the signal efficiency is 16.8% and the signal to background ratio, S/B, amounts to 1/300.

The selection is designed to optimise the statistical significance $S/\sqrt{S+B}$ for an integrated luminosity of $\mathcal{L} = 1\,\text{fb}^{-1}$. The first step of the selection requires a topology of $6 \leq N_{jet} \leq 8$. For a jet to be counted, the jet pseudorapidity must satisfy $|\eta| < 2.4$ and its transverse energy must be greater than 30 GeV. Event shape variables, potentially able to separate the signal from the background are then taken into account. The useful ones are centrality, aplanarity and non-leading jet total transverse energy obtained removing the two most energetic jets ($\sum_3 E_{\text{T}}$) of which distributions are shown in Figure 8.4. After the selection b-tagging is applied to the surviving samples of $t\bar{t}$ fully hadronic and QCD events. Selection criteria of at

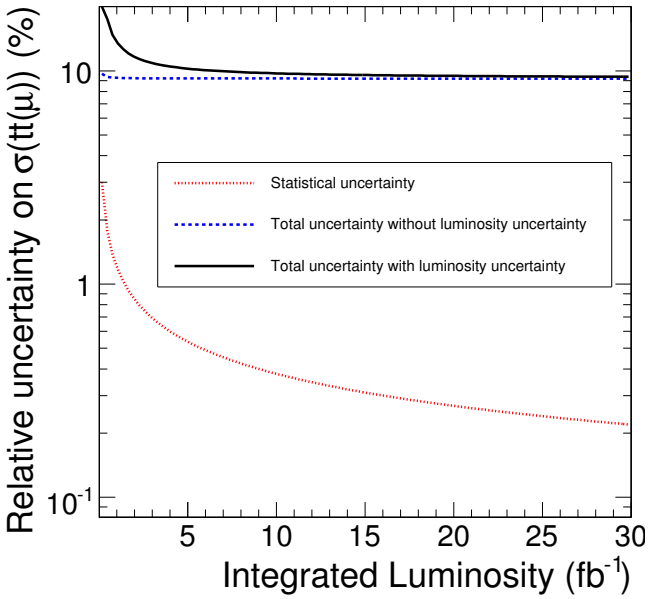

Figure 8.3: Statistical and total uncertainty on the inferred cross section of the process $pp \rightarrow t\bar{t} \rightarrow bq\bar{q}b\mu\nu_\mu$ as a function of the integrated luminosity.

least one b-jet and two b-jets are considered.

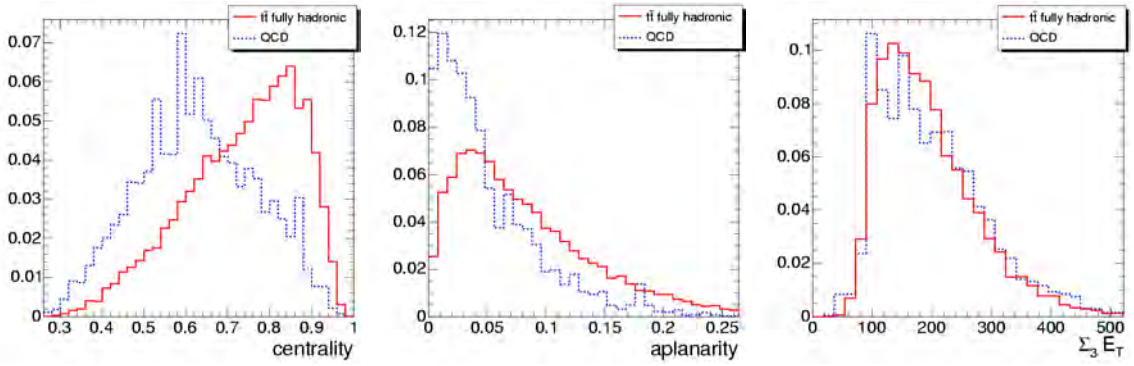

Figure 8.4: Distributions of centrality, aplanarity and $\sum_3 E_{\mathrm{T}}$ for $t\bar{t}$ and QCD events (normalised to the same area).

Table 8.6 summarises the selection applied in cascade. The signal-to-background ratio amounts to 1/17 and 1/9 for the 1 and 2 b-tag samples,respectively, and resulting in signal efficiencies of 3.8% and 2.7%.

The signal efficiency relative to the total inclusive $t\bar{t}$ sample, to be used in the calculation of the total $t\bar{t}$ production cross section, becomes 2.3% (1.6%), respectively for the 1 (2) b-tag requirement. The estimated statistical uncertainty on the cross section is reported in Table 8.7.

Sources of systematic uncertainty are studied as described in detail in [200] and [7]. From the experience of CDF and DØ experiments at Tevatron [290], one of the dominating systematic uncertainties arises from jet energy scale. The systematic uncertainty related with the trigger selection is calculated considering contributions from b-tagging and jet energy scale. Table 8.8 summarises the contributions to the total uncertainty on the cross section, which

Table 8.6: $t\bar{t}$ fully hadronic and QCD effective cross sections, signal-to-background ratio, statistical significance for 1 fb^{-1} and signal efficiency at each step of the selection.

Selection	Requirement	$\sigma\epsilon$ [pb]	$\sigma\epsilon_{\mathrm{QCD}}$ [pb]	S/B	$S/\sqrt{S+B}$	ϵ (%)
Before Selection (PYTHIA LO)		225	25M	$1/10^5$	0.04	100
Trigger	HLT multi-jet+b-jet	38	11600	1/300	11.1	16.8
Event	$6 \leq N_{jet} \leq 8$	35	7900	1/225	12.4	15.5
	$E_{\mathrm{T}} \geq 30$ GeV	15	930	1/60	15.4	6.6
	centrality ≥ 0.68	9.9	324	1/33	17.1	4.4
	aplanarity ≥ 0.024	9.0	251	1/28	17.7	4.0
	$\sum_3 E_{\mathrm{T}} \geq 148$ GeV	9.0	229	1/25	18.4	4.0
b-tagging	1 b-tag	8.6	148	1/17	21.7	3.8
	2 b-tag	6.0	54	1/9	24.1	2.7

Table 8.7: Number of $t\bar{t}$ and QCD events, $t\bar{t}$ efficiency, absolute and relative statistical uncertainties expected on the cross section measurement for an integrated luminosity of 1 fb^{-1}.

Requirement	$\mathcal{L} = 1$ fb^{-1}				
	$t\bar{t}$ events	QCD events	ϵ (%)	$(\Delta\sigma)_{stat}$ [pb]	$(\Delta\sigma/\sigma)_{stat}$ (%)
1 b-tag	11500	148000	2.3	17	3.5
2 b-tag	8000	54000	1.6	15	3.0

combined lead to a relative uncertainty of $\Delta\sigma/\sigma = 3\%(stat) + 20\%(syst) + 5\%(luminosity)$.

Table 8.8: Contributions to the systematic uncertainty on the $t\bar{t}$ cross section measurement in the fully hadronic channel (cut based approach).

	$\Delta\sigma/\sigma$ (%)
HLT	5.9
Pile Up	10.0
Underlying Event	4.1
Fragmentation	1.9
PDF	4.2
IS/FS Radiation	7.9
Jet Energy Scale	11.2
b-tagging	2.0
Background	5.0
Integrated Luminosity	5.0

8.1.4.2 Event selection based on neural net

A more refined selection is based on a neural net exploiting the same variables considered so far. Such approach is attempted in order to investigate the possibility of improving the S/B ratio and/or the efficiency. The previous selection, called "cut-based", could represent a more conservative approach for the first LHC analyses.

The most effective neural network configuration studied is applied to the $t\bar{t}$ and QCD events satisfying the topology request of $6 \leq N_{jet} \leq 8$ (jet pseudorapidity $|\eta| < 2.4$) after a cut on jet transverse energy of $E_{\mathrm{T}} > 25$ GeV and consists of 6 input nodes: E_{T} of the first and sixth jet with the jets ordered in increasing E_{T}, centrality, aplanarity, $\sum_3 E_{\mathrm{T}}$ and sphericity. The

performance of the neural net is shown in Figure 8.5 which compares the output distributions for signal and QCD background. The S/B ratio as a function of the $t\bar{t}$ efficiency is also shown. With respect to the cut-based selection, the request for a neural net output ≥ 0.77 improves the S/B ratio from 1/25 to 1/10 with same efficiency of about 4%.

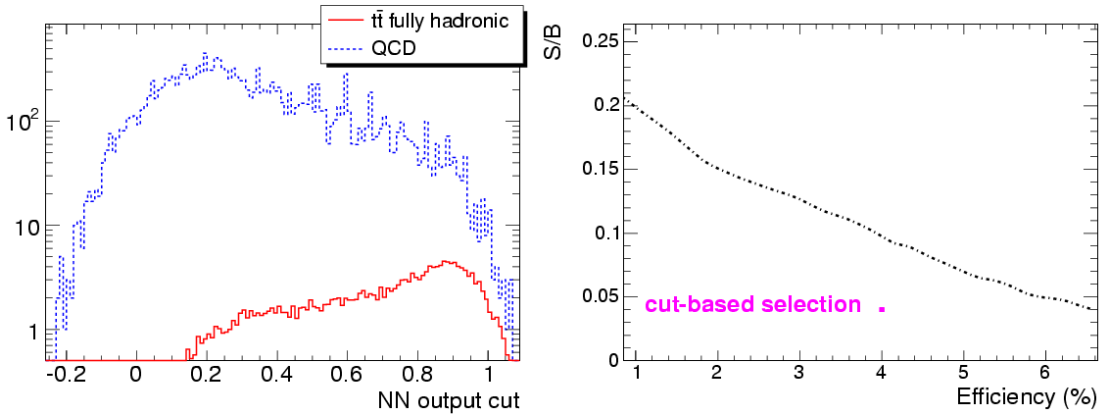

Figure 8.5: Left: distribution of the neural net output for $t\bar{t}$ and QCD. Right: signal-to-background ratio as function of the signal efficiency. For comparison the result of the cut-based selection is also shown.

As done after the cut-based selection, a b-tagging is applied to the surviving samples of $t\bar{t}$ fully hadronic and QCD events, and selection criteria of at least one b-jet and two b-jets are considered. Improved signal-to-background ratio, amounting to 1/7 (1/3) respectively for 1 (2) b-tag samples, can be achieved using the neural net keeping the same signal efficiencies of 3.8% (2.7%). This means an estimated relative statistical uncertainty on the cross section of 2.3% (2.0%), with the same expected number of $t\bar{t}$ events for an integrated luminosity of $\mathcal{L} = 1\,\text{fb}^{-1}$.

8.2 Measurement of the top quark mass

8.2.1 Dileptonic events

The dilepton channel benefits of a clean signature and a large signal-to-background ratio even though the presence of two neutrinos prevents a direct reconstruction of the top-quark mass. However, the event kinematic retains a large sensitivity to the top mass which can be exploited in various ways. The method presented here is discussed in more detail in [278].

The six unmeasured kinematic quantities corresponding to the momentum components of the two neutrinos are reduced by assuming momentum balance in the transverse plane, by imposing the m_W constraint and by requiring both top-quark masses to be equal. The event kinematics can then be written as a fourth order polynomial with the top mass as a parameter. For each candidate event we step through top mass values in the range $100\,\text{GeV/c}^2 \leq m_t \leq 300\,\text{GeV/c}^2$ in $1\,\text{GeV/c}^2$ steps and weight the kinematic solutions, including their four-fold ambiguity, with the Standard Model expectations of the neutrino momentum spectrum. For each event the most likely solution, i.e. the solution with the highest weight, is retained. The mass distribution of these most likely solutions is shown in Figure 8.1 for $1\,\text{fb}^{-1}$. The figure shows a clear mass peak at the expected value for the fully-simulated and reconstructed events. A Gaussian fit to the signal in a range corresponding to 40% of the maximum yields $m_t = 178.5 \pm 1.5\,\text{GeV/c}^2$ for an input top mass of $175\,\text{GeV/c}^2$, where the uncertainty is statis-

tical. With $10\,\text{fb}^{-1}$ the statistical uncertainty will be reduced to $0.5\,\text{GeV/c}^2$. The background is small and essentially flat and does not affect the mass determination significantly.

The main systematic effects are due to the assumptions used to reduce the complexity of the kinematic equation system and to detector effects. The dominating systematic effect in the first category is the uncertainty on the initial and final-state radiation which changes the amount of transverse momentum of the $t\bar{t}$-system and the kinematic constraints. This results in an uncertainty on the top mass of $\Delta m_t = 0.3\,\text{GeV/c}^2$ [200]. The zero width approximation for both the W bosons and the top quarks in the equation system gives rise to another shift of about $0.1\,\text{GeV/c}^2$.

The expected uncertainty on the jet energy scale for the early data amounts to 15%, independent of the jet p_T, which corresponds to an uncertainty of $\Delta m_t = 4.2\,\text{GeV/c}^2$ for the first $1\,\text{fb}^{-1}$ of integrated luminosity. This uncertainty is reduced to $2.9\,\text{GeV/c}^2$ with an improved calibration in $1 - 10\,\text{fb}^{-1}$ based on photons and jets, especially jets from W-boson decays in semi-leptonic and fully-hadronic $t\bar{t}$ events. Further improvement in the knowledge of the jet energy scale after $10\,\text{fb}^{-1}$ are expected to reduce this uncertainty to about $1\,\text{GeV/c}^2$.

In conclusion, the kinematic reconstruction of the dilepton channel will allow an early measurement of the top-quark mass. Assuming that the goal for a precise jet energy scale determination for b-quarks can be achieved the expected precision on the top mass in this channel with $10\,\text{fb}^{-1}$ is $\Delta m_t = 0.5\,\text{GeV/c}^2\ (stat) \pm 1.1\,\text{GeV/c}^2 (sys)$.

8.2.2 Semi-leptonic events

The semi-leptonic $t\bar{t}$ decay is traditionally called the *golden channel* for measuring the top-quark mass. A measurement based on advanced analysis tools is described in detail in [291]. The event reconstruction and initial event selection follows the one of Section 8.1.3. For the event to be selected, exactly two out of the four leading jets are b-tagged and the other two need to be anti-b-tagged. The four leading jets should not overlap in order to reduce ambiguities in the jet energy scale calibration procedure. The efficiency of each sequential cut is shown in Table 8.9.

Table 8.9: Overview of the selection criteria applied after the lepton cut $p_\text{T}^{lepton} > 20\,\text{GeV/c}$ in Table 8.4.

	Signal	Other $t\bar{t}$	W+4j	Wbb+2j	Wbb+3j	S/B
Before selection	365k	1962k	82.5k	109.5k	22.5k	0.032
b-tag criteria	5.5%	0.21%	0.052%	0.47%	0.70%	3.73
No jet overlap	3.0%	0.11%	0.027%	0.25%	0.44%	3.87
P_{χ^2}-cut 20%	1.4%	0.039%	0.0097	0.061	0.07	5.3
P_{sign}-cut 80%	1.2%	0.025%	0.0085	0.052	0.05	6.8
P_{comb}-cut 50%	0.7%	0.013%	0.0036	0.013	0.	8.2
Scaled $\mathcal{L} = 1\,\text{fb}^{-1}$	588	64	6	2	0	8.2

The amount of events produced via a different $t\bar{t}$ decay channel in the selected event sample is reduced by a likelihood-ratio method combining three kinematic observables resulting in a variable L_{sign} which is transformed into a probability P_{sign} for the selected event to be a semi-leptonic muon $t\bar{t}$ event. An extra sequential cut is applied by requiring this probability P_{sign} to exceed 80%.

Among the four reconstructed jets, three have to be chosen to form the hadronic decaying top quark. The efficiency and purity of this selection was significantly enhanced by applying a second likelihood ratio method combining the information from several sensitive variables. The jet combination with the largest L_{comb} value is taken as the best pairing. The L_{comb} value is transformed into a probability P_{comb} for the chosen combination to be the correct one. The event probability P_{comb} is used in the event selection where events are selected if their value for P_{comb} exceeds 60%, increasing the purity of the selected jet pairings to 81.6% in the mass window of $25\,\mathrm{GeV/c^2}$ around the expected m_t of about $175\,\mathrm{GeV/c^2}$.

For each jet combination a kinematic fit was applied as described which imposes the W-boson mass for the hadronically-decaying W boson in the event [166]. Only jet combinations are considered with a probability of the kinematic fit calculated from its χ^2/ndf exceeding 20%. For some events none of the jet combinations fulfill this criterium, therefore reducing the total event selection efficiency. The fraction of fully hadronic $t\bar{t}$ events selected is negligible (less than 0.05 events expected at $1\,\mathrm{fb}^{-1}$). Form this we conclude that the also influence of QCD produced jet events is minor.

When estimating m_t from the selected event sample by a simple Gaussian fit in a range of $20\,\mathrm{GeV/c^2}$ in both directions around the modal bin, a value of $176.5 \pm 0.65\,\mathrm{GeV/c^2}$ is obtained before applying the kinematic fit and $172.2 \pm 0.48\,\mathrm{GeV/c^2}$ after applying the kinematic fit, for an input value of $175\,\mathrm{GeV/c^2}$. The errors reflect the statistical precision of the available Monte Carlo signal sample. The top quark mass after the kinematic fit is shown in Figure 8.6.

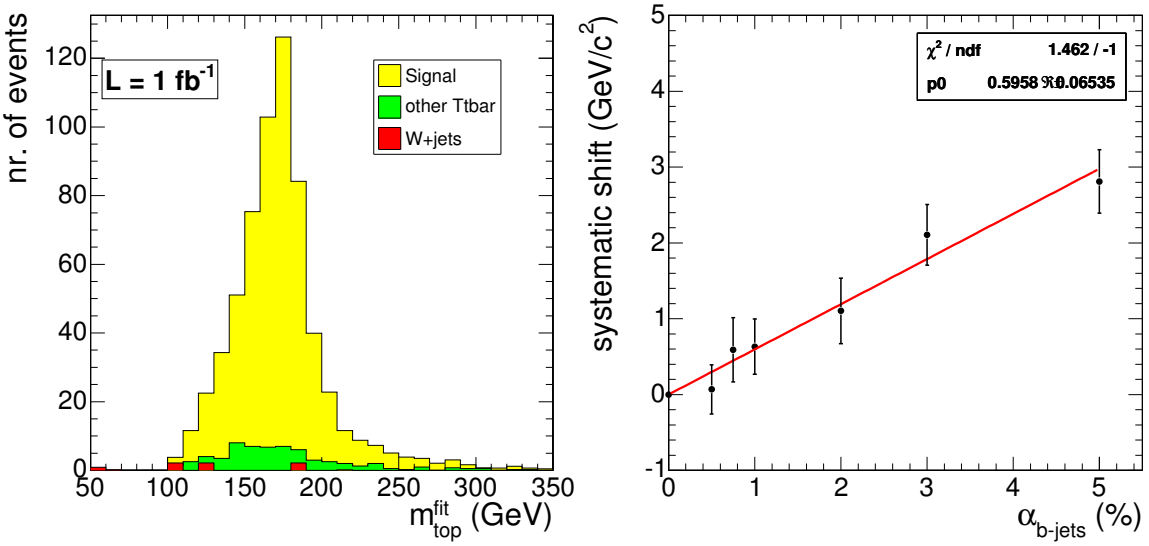

Figure 8.6: Left: Distribution of the mass of the hadronic decaying top quark for the selected events after applying the kinematic fit. Right: Estimated shift in $M_t^{FullIdeo}$ versus a relative shift α applied on the inclusive heavy quark jet energy scale.

Rather than developing m_t estimators on samples of events, an event-by-event likelihood approach is used to estimate m_t from the fitted kinematics of the three jets of the hadronically decaying top quark. The uncertainty on m_t for each event is determined from the covariance matrices of the kinematic fit. This uncertainty can either be assumed Gaussian or the full m_t range can be explicitly scanned with the kinematic fit.

To obtain information about the true value of M_t we convolute the reconstructed resolution function or ideogram with the theoretical expected probability density function $P(m_t|M_t)$ in

the reconstruction space

$$\mathcal{L}_i(M_t) = \int P(\{\overline{p}_j\}|m_t) \cdot P(m_t|M_t)\, dm_t \tag{8.1}$$

where one integrates over the kinematic relevant range of m_t to obtain a likelihood function $\mathcal{L}_i(M_t)$ for each event i. Several contributions are added in the expected density $P(m_t|M_t)$: a Breit-Wigner shape for the correct jet combinations $S(m_t|M_t)$, a parameterised combinatorial background contribution $B_{comb}(m_t)$ and a parameterised background contribution $B_{proc}(m_t)$. This results in a function

$$P(m_t|M_t) = P_{sign} \cdot [P_{comb} \cdot S(m_t|M_t) + (1 - P_{comb}) \cdot B_{comb}(m_t)] + (1 - P_{sign}) \cdot B_{back}(m_t) \tag{8.2}$$

where each contribution is weighted according to the probabilities extracted from the observed event. After combining the likelihoods $\mathcal{L}_i(M_t)$ from all selected events, a maximum likelihood method is applied to obtain the best value for the estimator $\hat{M}_t$.

The linearity of the estimators have been checked and the slopes are found to be compatible with unity. The width of the pull distribution of the top quark mass estimators $\hat{M}_t$ are found to be 0.82 for $\hat{M}_t^{fit}$ (simple fit on reconstructed mass spectrum), 1.04 for $\hat{M}_t^{ParIdeo}$ (convolution with the parameterised ideogram) and 1.02 for $\hat{M}_t^{FullIdeo}$ (convolution with the full scanned ideogram). The resulting top quark mass for the estimator $\hat{M}_t^{fit}$ applied on the simulated events samples with a generated top quark mass of $175\,\text{GeV/c}^2$ is $174.16 \pm 0.59\,\text{GeV/c}^2$, hence reflecting a bias of $-0.84\,\text{GeV/c}^2$. For the convolution method this is $170.65 \pm 0.54\,\text{GeV/c}^2$ and $172.42 \pm 0.31\,\text{GeV/c}^2$ for respectively the $\hat{M}_t^{ParIdeo}$ and the $\hat{M}_t^{FullIdeo}$ estimator. Figure 8.7 illustrates the results.

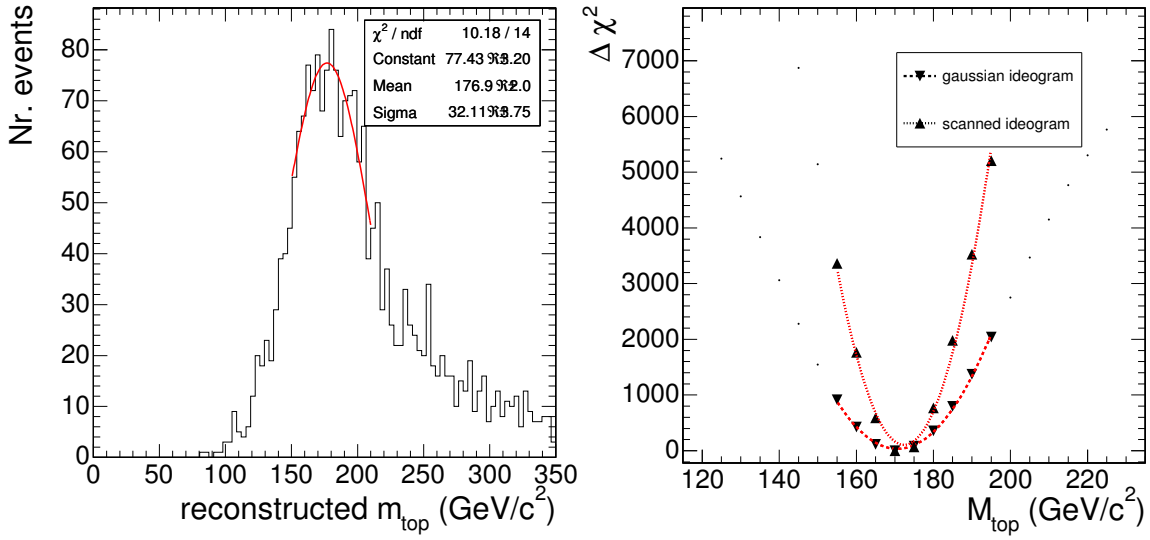

Figure 8.7: Distribution of the mass of the hadronic decaying top quark before the kinematic fit used for the $\hat{M}_t^{fit}$ estimator (left) and the combined $\Delta\chi^2(M_t)$ function over all events for both ideogram based estimators $\hat{M}_t^{ParIdeo}$ and $\hat{M}_t^{FullIdeo}$ (right).

Several systematic effects introduce an uncertainty on the top quark mass estimator. They originate from our understanding of the detector performance, the robustness of the reconstructed objects, for example jets, and the general description of the proton collisions in the

simulation. A full description can be found in [291]. The estimation of the systematic uncertainties follows that of the cross section measurement in Section 8.1.3. We conservatively conclude that a total precision on the top quark mass of $1.9\,\mathrm{GeV/c^2}$ can be reached with $10\,\mathrm{fb}^{-1}$ of data. The uncertainty is dominated by systematic effects like pile-up collisions and the knowledge of the jet energy scale of b-quark jets (see Figure 8.6).

After achieving a better understanding of the accelerator settings and the detector performance, however, the total uncertainty will decrease. Our understanding of the underlying event model will improve in the future significantly when new tuning data become available. The magnitude of pile-up collisions could be monitored to the level of 10%. To take into account the overlap between the pile-up and the jet energy scale uncertainty, the systematic shift due to a 10% variation in the pile-up collisions is divided by two. The uncertainty on the energy scale of b-quark jets can be extrapolated to about 1.5% after a better understanding of the detector performance and with the application of advanced tools like energy flow algorithms or selecting jets only in well understood regions in the detector. The measurement of the b-tag efficiency [285] is dominated by systematic uncertainties of radiation effects. The experience at the Tevatron collider [287, 288] illustrates that an uncertainty of 2% could be reached.

Table 8.10: Overview of all uncertainty components on the top quark mass estimators, extrapolated to a better understanding of both the proton collisions at the LHC and the detector performance.

	Standard Selection		
	Gaussian Fit Δm_t ($\mathrm{GeV/c^2}$)	Gaussian Ideogram Δm_t ($\mathrm{GeV/c^2}$)	Full Scan Ideogram Δm_t ($\mathrm{GeV/c^2}$)
Pile-Up (5%)	0.32	0.23	0.21
Underlying Event	0.50	0.35	0.25
Jet Energy Scale (1.5%)	2.90	1.05	0.96
Radiation (Λ_{QCD}, Q_0^2)	0.80	0.27	0.22
Fragmentation (Lund b, σ_q)	0.40	0.40	0.30
b-tagging (2%)	0.80	0.20	0.18
Background	0.30	0.25	0.25
Parton Density Functions	0.12	0.10	0.08
Total Systematical uncertainty	3.21	1.27	1.13
Statistical Uncertainty ($10\,\mathrm{fb}^{-1}$)	0.32	0.36	0.21
Total Uncertainty	3.23	1.32	1.15

Table 8.10 summarises and combines the extrapolated systematic uncertainties on each of the top quark mass estimators. The uncertainty on the inferred top quark mass of about $1.2\,\mathrm{GeV/c^2}$ is dominated by the uncertainty on the energy scale of the b-quark jets. This relative uncertainty is taken to be 1.5% which defines a goal for the performance of jet calibration methods.

8.2.3 Fully hadronic events

The selection described in Section 8.1.4.1, including the demand for the two b-tags, forms the basis for a selection of fully hadronic $t\bar{t}$ events suitable for a kinematic top-mass reconstruction. An additional cut on the two leading jets, $100\,\mathrm{GeV/c} < p_\mathrm{T} < 300\,\mathrm{GeV/c}$, is effective against background from mis-reconstructed events and combinatorial background.

The six partons in $pp \rightarrow t\bar{t} \rightarrow bW^+\bar{b}W^- \rightarrow bq_1\bar{q}_1'\bar{b}q_2\bar{q}_2'$ are matched to six reconstructed jets by picking the matching which minimises the sum of the angular separation between reconstructed jet and matched parton. Only jets satisfying our initial jet-definition, $p_{\mathrm{T}} > 30\,\mathrm{GeV/c}$ and $|\eta| < 2.4$, as employed in the selection, are taken into account in the matching process. Based on the amount of the angular separation three disjunctive classes of signal events are defined: good (36%), half-good (45%) and bad jet-parton-matching (19%). The first class being the events where all six partons are matched well by jets, the second class where only the three partons from one top are matched well by jets. The reason for the mismatch can be traced to parton-level properties, like high $|\eta|$ and low p_{T}, described in more detail in [278].

In order to perform the correct jet pairing, a likelihood variable is constructed from the following event observables: (a) average of the two W-boson masses, (b) difference of the two W-boson masses, (c) sum of the inter-jet angles of the W-boson candidates $\angle(q_1\bar{q}_1') + \angle(q_2\bar{q}_2')$, (d) difference of the two top-quark masses, (e) sum of the inter-jet angles of the top quark candidates $\angle(bq_1) + \angle(b\bar{q}_1') + \angle(q_1\bar{q}_1') + \angle(\bar{b}q_2) + \angle(\bar{b}\bar{q}_2') + \angle(q_2\bar{q}_2')$, (f) angle between the direction of the two top-quark candidates. Their distributions are shown in [278]. Taking for each event the pairing with the highest likelihood value yields pairing efficiencies of 71% for the good and 64% for the half-good jet-parton-matching.

Only one top per event is chosen for the kinematic mass determination, the choice is once again based on a likelihood variable constructed from the following event observables: (a) p_{T} of the softest of the three jets of each top-quark candidate (b) mass of the W boson as reconstructed in top decay (c) sum of the inter-jet angles of jets from top decay, $\angle(b_iq_i) + \angle(b_i\bar{q}_i') + \angle(q_i\bar{q}_i')$. Taking the top with the larger likelihood value yields a 72% efficiency, far greater than the 50% efficiency of a random choice.

The differentiation of the selected signal events into the now six classes is summarised in Table 8.11, where the six classes are being mapped onto two labels, indicating whether the events are considered signal- or background-like.

Table 8.11: Distribution of the different signal event classes after jet-pairing and top-choice in the $t\bar{t}$ fully hadronic channel. The label column indicates whether the class is considered signal- or background-like.

reconstruction	pairing	[pb]	top-choice	[pb]	label
good	correct	0.62 (35%)	always correct	0.62 (35%)	sig.
	wrong	0.26 (14%)	always wrong	0.26 (14%)	bkg.
half-good	correct	0.46 (25%)	correct	0.33 (18%)	sig.
			wrong	0.13 (7%)	bkg.
	wrong	0.26 (15%)	always wrong	0.26 (15%)	bkg.
bad	always wrong	0.20 (11%)	always correct	0.20 (11%)	bkg.

With all the pieces in place a kinematic reconstruction of the top quarks is straightforward and the resulting invariant mass distribution of the chosen top, with the paired non-b-jets rescaled such that they yield the W-mass, is shown in Figure 8.8.

As expected the signal-like events form a narrow peak, while the wrongly-reconstructed events have a far broader shape. Fitting a Gaussian to the peak of the invariant mass distributions with a fit range corresponding to 0.4 of the peak maximum, as shown in Figure 8.8 serves as a simple mass estimator. The extracted top-mass is $m_t = 175.0 \pm 0.6\,(\mathrm{stat.}) \pm 4.2\,(\mathrm{syst.})\,\mathrm{GeV/c^2}$ for an input top-mass of 175 $\mathrm{GeV/c^2}$ and an integrated luminosity of $\mathcal{L} =$

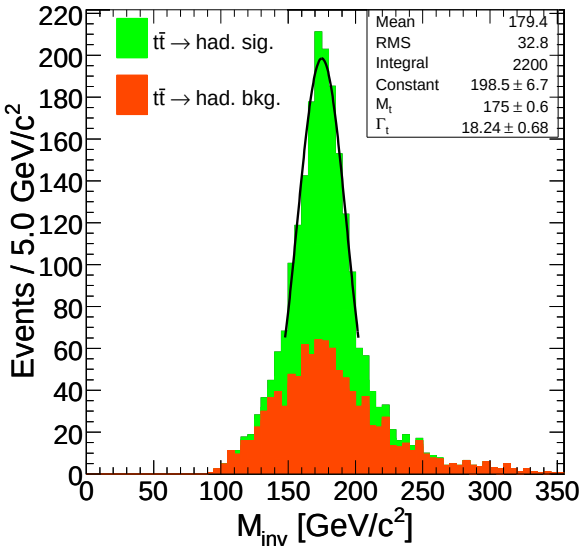

Figure 8.8: Invariant mass distribution of the reconstructed and rescaled, chosen top for both signal classes with a Gaussian fit to the peak.

$1\,\mathrm{fb}^{-1}$.

Table 8.12: Summary of the systematics for the top-mass determination with fully hadronic events.

	$\Delta m_t[\mathrm{GeV/c^2}]$
Pile Up	0.4
Underlying Event	0.6
PDF	1.4
IS/FS Radiation	2.3
Fragmentation	0.9
Jet Energy Scale	2.3
b-Tagging	0.3
Background	2.0

Already with this amount of data the statistical error becomes negligible compared to the systematic uncertainties which are summarised in Table 8.12. One of the big systematic uncertainties is the QCD background. The S/B in the displayed mass window of Figure 8.8 is about $2/3$, although not shown since the currently available number of simulated events does not allow a determination of the QCD background shape and of the uncertainty it introduces into the top-mass determination. Experience from CDF at the Tevatron [292, 293] indicates that this uncertainty can be understood at the $\sim 2\,\mathrm{GeV/c^2}$ level, when using data for background estimation.

8.2.4 Top quark mass from J/ψ final states

8.2.4.1 Introduction

At the LHC the measurement of the top quark mass via direct reconstruction will soon be limited by systematic errors. It is expected that the most severe systematic contributions will be linked to the modelling of the hadronic environment and the knowledge of the jet energies. It would be particularly desirable, therefore, to consider methods for the extraction of

m_t from the data which could reduce the contribution from these uncertainties considerably. An alternative method, which is making use of exclusive b decays in semi-leptonic top-pair events with the presence of a J/ψ decaying into an electron or muon pair was proposed in [294, 295].

The top quark mass is determined by its correlation with the invariant mass of the reconstructed J/ψ and the lepton from the W decay coming from the same top decay, $\mathrm{m_{J/\Psi\ell}}$. The correlation is present because the reconstruction of the J/ψ gives an accurate measurement of the b quark flight direction and its momentum thanks to the relatively high mass of the meson. Moreover, this measure is expected to have an excellent resolution because of the very clean experimental reconstruction of the lepton three-vectors. Details on the analysis presented here can be found in [296].

8.2.4.2 Event generation and selection

Signal events are generated using the TOPREX generator [44] and consist of $t\bar{t}$ events where the presence of at least one J/ψ in the final state from the hadronisation of b-quarks is required. No distinction is made about the origin of the J/ψ; therefore the same samples also contains combinatorial background where the J/ψ is coming from a b quark produced together with a W boson decaying hadronically. Five samples corresponding to five different top masses are generated with a statistics of 200K events each. The event hadronisation and the description of the underlying event and the minimum bias is realised with PYTHIA 6.227 [24].

All the signal samples are passed through full detector simulation (ORCA) [10] with a simulation of the minimum bias corresponding to high luminosity data taking. Indeed, the statistics is expected to be so low that the use of high luminosity data must be considered. The same signal samples, and several millions more for studies on systematics, are passed through the fast simulation of the detector (FAMOS) [11]. The shape of the variables used in the selections are fully compatible in both scenarios.

The studied physics backgrounds are generated with the ALPGEN [160] generator and include $W + \mathrm{jets}$, $Zb\bar{b} + \mathrm{jets}$, $Wb\bar{b} + \mathrm{jets}$. In these cases the samples are not biased by requiring an explicit J/ψ in the final state, therefore the separation from the signal is studied on the basis of cuts not involving the search for a J/ψ and the contribution of the resulting background is then rescaled taking into account the proper branching fractions. The selection, in terms of signal efficiency, is also cross-checked against $t\bar{t} + \mathrm{jets}$ signal generated with ALPGEN, and is found to be consistent.

The main difficulty of the analysis comes from the extremely low branching ratio for a $t\bar{t}$ event to give a final state with a leptonic J/ψ. This can be written as:

$$\begin{aligned} BR(t\bar{t} \to (Wb)(Wb) \to (Xb)(\ell\nu J/\psi X)) \;&=\; 2 \cdot BR(W \to \ell\nu) \\ \cdot BR(b(\to X) \to B^{\pm,0}, B_s, B_{baryon} \to J/\psi X) &\cdot BR(J/\psi \to \ell\ell) \end{aligned} \tag{8.3}$$

where charge conjugation is implicit, ℓ indicates either an electron or a muon, and having assumed a $BR(t \to Wb)$ of 1. Replacing the branching ratios with up-to-date numbers [54] one gets for the global branching ratio the value $5.5 \cdot 10^{-4}$ that, in terms of event yield and assuming a cross section for $pp \to t\bar{t}$ of 830 pb, makes approximately 4500 events per $10\,\mathrm{fb}^{-1}$. This number does not include neither the trigger and selection efficiency, nor the efficiency for the correct pairing of the J/ψ to the correct lepton from the W decay.

Events are triggered using the inclusive lepton trigger with thresholds described in [75]. The efficiency for triggering signal events is reported in Table 8.13 and is included in all numbers presented here. In events passing the trigger thresholds a J/ψ is searched for by looking for same-flavour, opposite-sign leptons with invariant mass in the range [2.8,3.2] GeV/c^2 and forming an angle greater than 2 and lower than 35 degrees. No isolation requirements must be imposed on these leptons. The efficiency for reconstructing a J/ψ at this stage is (0.386 ± 0.007) and (0.114 ± 0.004) for the muon and electron channels, respectively. It is limited by the low momenta of the leptons and because they are produced inside a jet, making the reconstruction more difficult, particularly for electrons.

If a J/ψ is found in an event, the isolated lepton with the highest p_{T} and higher than 20 GeV/c is considered as the lepton candidate from the W decay. The isolation discriminant is defined as the sum of the energies in the electromagnetic and hadronic calorimeters in a cone of opening angle $\Delta R = 0.3$ around the lepton candidate. The selection requires that the isolation energy is less than 15 GeV for electrons and less than 20 GeV for muons.

We define as background all contributions from processes not resulting in the decay chain $t \to Wb \to \ell\nu J/\psi X$. We call physics background the contribution from processes other than $t\bar{t}$ (semi)leptonic and as combinatorial background the irreducible part of $t\bar{t}$ (semi)leptonic where the J/ψ is wrongly associated to the lepton not coming from the W in the same top decay. Any physics background needs to mimic a final state with the presence of a J/ψ and an isolated and energetic lepton. The obvious candidates are bosons in association with jets. It is important to distinguish between b jets and light jets, which produce J/ψ at very different rates, suppressing the contribution of processes with light jets very much. To remove these contributions the total scalar sum of the transverse jet momenta is required to be greater than 100 GeV/c. This cut is not applied if two isolated leptons are found, in order to preserve dileptonic $t\bar{t}$ events. If the flavour of the two leptons is the same, an explicit cut to remove the presence of leptonic Z is made, vetoing events where the invariant mass of the two leptons is between 85 and 97 GeV/c^2. To further reduce soft background the cut on the transverse momentum of the isolated lepton is brought to 40 GeV/c, making the analysis less sensitive also to systematic effects involving soft QCD. Table 8.13 presents, in terms of predicted cross sections, efficiencies and events yields per $10\,\mathrm{fb}^{-1}$, the performance of the analysis.

8.2.4.3 Reconstruction of $\mathrm{m}_{\mathrm{J}/\Psi\ell}$ and statistical performance

In order to estimate the correct invariant mass J/ψ-lepton it would be necessary to efficiently discriminate between right pairings, where both particles are coming from the decay of the same top, and from wrong pairings where, in $t\bar{t}$ events, they come from the two different top decays. In the present analysis, in order to increase the available statistics, we propose not to attempt any separation of the combinatorial but, instead, to use the full distribution containing both signal and background.

Figure 8.9 shows the three-lepton invariant mass in $t\bar{t}$ events at generator level without selection and at full reconstruction after the selection described in the previous section. The distribution of the components of signal and background from $t\bar{t}$ are shown, where the Monte Carlo truth is used to judge when the correct pairing is made. No equivalent distribution can be done for non-$t\bar{t}$ backgrounds since no J/ψ is present in those samples. To take this into account the pure background shape is scaled up according to the extra contribution of non $t\bar{t}$ background (Table 8.13), in the hypothesis that the shape of the two samples are the same. Uncertainty in the background description will then be translated into a systematic

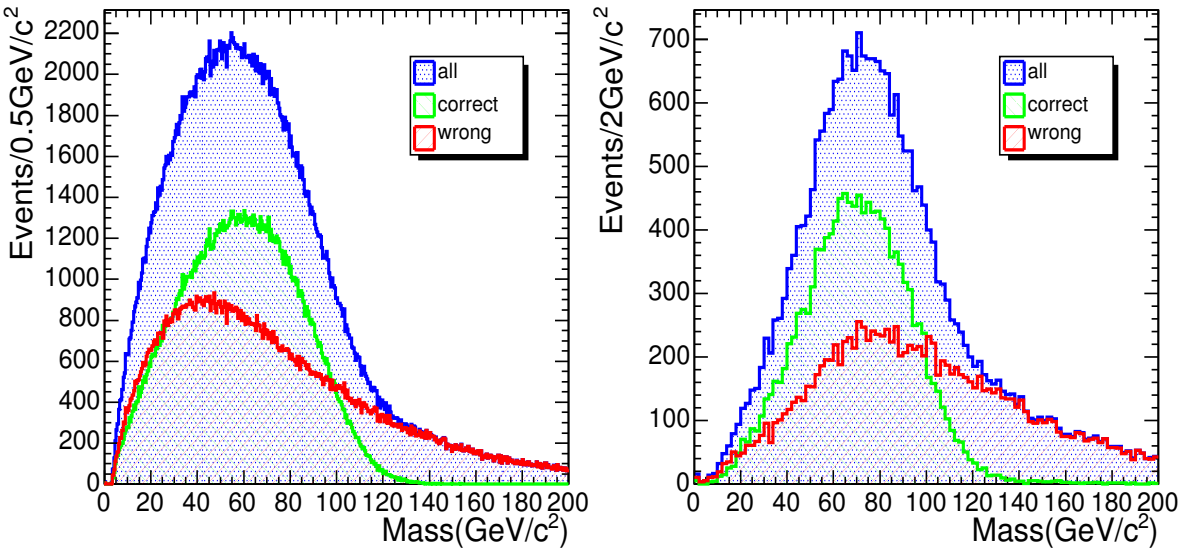

Figure 8.9: Three-lepton mass distribution for $m_t = 175\,\text{GeV/c}^2$ at generator level (left) and after detector simulation and reconstruction (right). In the pictures the components coming from correct and wrong lepton pairing - from both combinatorial and physics backgrounds - are shown.

contribution on the measurement.

The observable most sensitive to the top mass is the position of the maximum of the three-lepton mass distribution. It is determined via a fit of the full shape with a polynomial function of fourth degree. The range chosen for the fit is centred around the maximum and goes

Table 8.13: Selection performance on signal and expected backgrounds. The first column indicates the channel and its final state, the second the predicted cross section, where the branching ratio for producing at least a J/ψ into leptons from either a b jet or a light jet is accounted for, the third the trigger efficiency, the fourth the selection efficiency, the fifth the expected number of events in $10\,\text{fb}^{-1}$, the sixth the classification of the contribution as signal (S), physics background (B) or combinatorial background (C).

Channel	BR·σ (fb)	ϵ_{trig} (%)	ϵ_{sel} (%)	Events in $10\,\text{fb}^{-1}$	Class
$t\bar{t} \to (b \to J/\psi)\ell\nu - b\ell\nu$	107	93.9	15.7±0.4	158	S+C
$t\bar{t} \to (b \to J/\psi)\ell\nu - b\tau\nu$	53	61.1	11.0±0.8	36	S
$t\bar{t} \to (b \to J/\psi)\ell\nu - bqq$	320	55.3	10.9±0.3	193	S
$t\bar{t} \to (b \to J/\psi)\tau\nu - b\ell\nu$	53	61.1	10.6±0.8	34	C
$t\bar{t} \to (b \to J/\psi)\tau\nu - b\tau\nu$	27	14.2	2.8±1.2	1	B
$t\bar{t} \to (b \to J/\psi)\tau\nu - bqq$	160	7.9	1.5±0.5	2	B
$t\bar{t} \to (b \to J/\psi)qq - b\ell\nu$	320	55.3	10.7±0.3	190	C
$t\bar{t} \to (b \to J/\psi)qq - b\tau\nu$	160	7.9	1.5±0.5	2	B
$t\bar{t} \to (b \to J/\psi)qq - bqq$	959	0.1	0.2±0.5	0	B
$W + N\,\text{jets}, N > 1 \to J/\psi X$	394	55.3	2.1±0.1	43	B
$Wb\bar{b} + \text{jets} \to J/\psi X$	196	55.3	1.6±0.1	16	B
$Zb\bar{b} + \text{jets} \to J/\psi X$	23	93.9	9.4±0.1	20	B
$b\bar{b} \to J/\psi X$	$1.3{\cdot}10^9$	$<2{\cdot}10^{-8}$	<1	<2.6	B

from 20 to 120 GeV/c^2. The error on the maximum of the fitted polynomial is determined by propagating the errors on the fitted coefficients and taking into account their correlation. As a cross check, an alternative way of fitting the signal with a gaussian was tried. In this case the background is first subtracted on a bin-by-bin basis making use of an average background distribution determined by using all the simulated samples. The results obtained are comparable.

The fitted maxima are expected to be correlated to the input value of the top mass. This correlation is proven and fitted by a line (Figure 8.10). The two results at fast and full simulation are in impressive agreement. The correlation curves can be used to estimate the

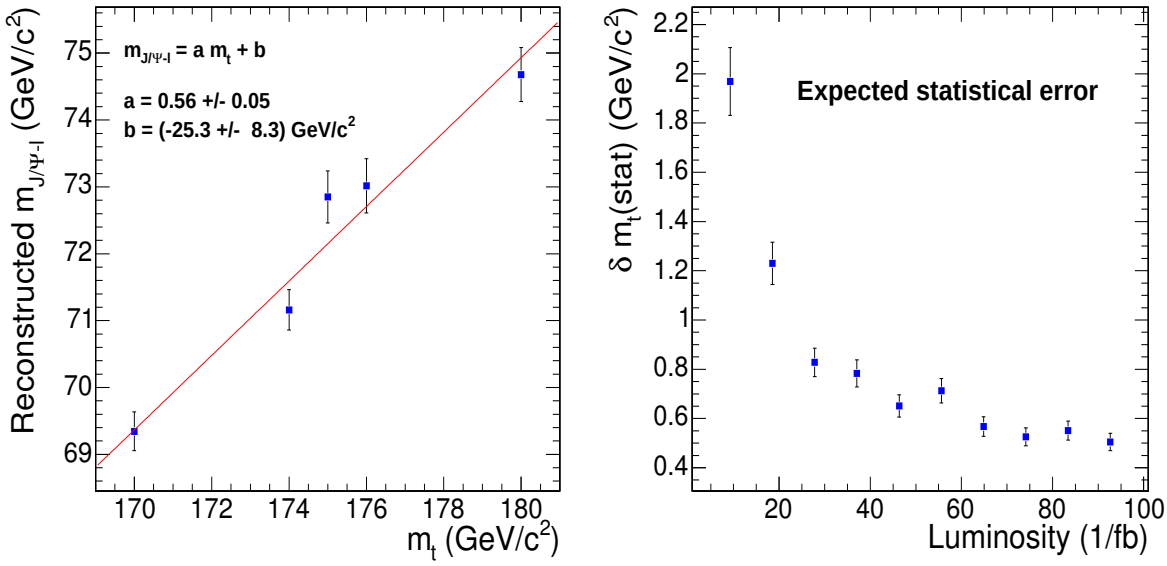

Figure 8.10: Left: correlation between the reconstructed three-lepton invariant mass and the input top mass at full simulation. Right: expected statistical error on the top quark mass as a function of the integrated luminosity.

expected statistical error on the top mass as a function of the available amount of data. This is done by using the number of events expected according to Table 8.13, and the result is presented in Figure 8.10. From the figure it can be concluded that the measurement of the top quark mass with this analysis can become, on the statistical footing, competitive already with other analyses' total error after the first years of data taking. Moreover the measurement is expected to be dominated by systematic errors in the long range, as explained in the next section.

8.2.4.4 Systematic errors

The sources of systematic errors can be divided into two main categories: theoretical and experimental. The former include the description of the hard process and the modelling of radiation, fragmentation and the underlying event in the simulation, whereas the latter includes all experimental sources coming from an imperfect detector description. The sources analysed in what follows are considered as uncorrelated and the corresponding resulting errors on the top mass are summed in quadrature to form the total systematic error. To evaluate the effect of various sources the guidelines described in [200] and in Appendix B are followed.

With the exception of the PDF description, for each of the other sources of theoretical uncertainty and for each change in the simulation parameters an independent signal generation with TOPREX and PYTHIA has been performed, with statistics of a few 100K events each, and fast simulated. The variations on the resulting top masses are considered as systematics: when the mass difference with respect to the reference sample is smaller than the associated statistical error, this is conservatively quoted as the systematic error.

For all the experimental sources, smearings and shifts on the observed objects (leptons and jets) are applied after reconstruction and before selection in a consistent way. The observed difference on the top mass is taken as an estimation of the associated systematic uncertainty.

Table 8.14 presents the systematic breakdown on the top mass. The systematics error is dominated by theoretical sources, which are the ones affected by the larger statistical uncertainties, quoted here as systematics.

Table 8.14: Systematic error breakdown. For each source either the maximum variation from a reference sample or the resulting statistical error on the difference is quoted as a systematic error.

Source	δm_t(GeV/c^2)
Λ_{QCD}	0.31
Q^2	0.56
Scale definition	0.71
b-quark fragmentation	0.51
Light jet fragmentation	0.46
Minimum bias/Underlying event	0.64
Proton PDF	0.28
Total theoretical	1.37
Electron E scale	0.21
Muon p scale	0.38
Electron E resolution	0.19
Muon p resolution	0.12
Jet E scale	0.05
Jet E resolution	0.05
Background knowledge	0.21
Total experimental	0.54
Total systematic	1.47

Putting together the systematic and the statistical error one can conclude that, with maybe exception for the first year of data taking, this measurement will be dominated by systematics, in turn dominated by our poor understanding of the theoretical sources. A total error on the top mass below 2 GeV/c^2 can be in reach from the first 20 fb^{-1} already. The present result suggests an uncertainty of 1.5 GeV/c^2 with full statistics, but this number is fully dominated by the theory systematics. A precision much better than this is not out of reach since, by the time this measurement will be made, the analysis will be hopefully repeated at (N)NLO and our understanding of the dominating systematics, for instance the minimum bias and the underlying event, will be drastically improved. More dedicated reconstruction techniques and more sophisticated analyses will considerably improve the statistical treatment of the information.

This analysis reduces to a minimum those systematics which are expected to dominate in

more traditional estimations of the top mass, especially the ones from direct reconstruction, like the jet energy scale and the knowledge of the b-tagging.

8.2.5 Summary of top mass determinations

Measuring the mass of the top quark in different channels allows for a combination of the individual results [297]. As the statistical component in the total uncertainty on m_t in each channel is negligible, the correlation between the systematic uncertainties must be determined. The dominant uncertainty arises from the knowledge of the energy scale of b-quark jets, a component which is assumed to be fully correlated between decay channels. This uncertainty can however be subdivided in several components: detector understanding, clustering algorithms, related to the modelling of b- and light-quark fragmentation and decay and, finally, the statistical precision of the data-based estimates of the b-jet energy scale differentiated versus the pseudo-rapidity and the transverse momentum of the observed jet.

The measurement from the J/ψ final states is however limited by other, mainly theoretical, sources of systematic uncertainties. Therefore a reduction of the uncertainty on m_t is expected when combining the direct measurements with the measurement from the J/ψ final states. The knowledge of the top quark mass can be improved by developing alternative methods which do not rely on the b-jet energy scale [298, 299]. Accounting for these future improvements an uncertainty of $1\,\mathrm{GeV/c^2}$ on the top quark mass is feasible. The combination can be performed by applying techniques described in [300, 301].

8.3 Spin correlation in top-quark pair production

8.3.1 Introduction

Because of its large width of $1.4\,\mathrm{GeV/c^2}$ the top quark decays before either hadronisation, governed by the scale Λ_{QCD}, or depolarisation, governed by the scale Λ^2_{QCD}/m_t, can take place. This unique feature is used to investigate the spin of the top quark; such investigation is not possible in the case of light quarks, where the spin information is diluted by hadronisation. Moreover, the top quark spin-flip time is much larger than its lifetime and the probability of a spin flip due to emission of one or several gluons via chromomagnetic dipole-transition is very small.

The angular distribution of a daughter particle in top quark decays can be written as [302–304]

$$\frac{1}{\Gamma}\frac{d\Gamma}{d\cos\theta_i} = \frac{1}{2}(1 + \kappa_i \cos\theta_i)\,, \tag{8.4}$$

where the decay angle θ_i is defined as the angle between the direction of motion of the daughter particle i and the chosen spin quantisation axis. As gluon fusion is the dominant production mechanism at the LHC there is no well defined spin axis in the initial state. This leads to a choice of the helicity basis along the top quark momenta in the partonic centre-of-mass frame. The spin-analyser quality κ of the top quark daughter particle is defined as the degree to which the daughter particle is correlated with the top-quark spin. The analysis presented here is based on the semi-leptonic $t\bar{t}$ decay channel with electrons or muons, which is considered to be the signal. Alternatively, the dileptonic $t\bar{t}$ decay channel can also be considered. The κ values for the daughter particles used in this analysis [305], lepton, b quark and the lower energy quark from W decay, are 1, -0.41 and 0.51, respectively.

The spin correlation in the semi-leptonic $t\bar{t}$ decay channel can be measured in terms of a double differential lepton and quark angular distribution, which, neglecting higher order QCD corrections, is given by

$$\frac{1}{N}\frac{d^2N}{d\cos\theta_l\, d\cos\theta_q} = \frac{1}{4}(1 - \mathcal{A}\kappa_l\kappa_q \cos\theta_l \cos\theta_q)\ . \tag{8.5}$$

Here, using the helicity basis the lepton and quark angles θ_l and θ_q are obtained by measuring the angle between the decay particle momentum in its parent top quark rest frame and the parent top quark momentum in the $t\bar{t}$ quark pair rest frame. The correlation coefficient

$$\mathcal{A} = \frac{N_{||} - N_X}{N_{||} + N_X} = \frac{N(t_L\bar{t}_L + t_R\bar{t}_R) - N(t_L\bar{t}_R + t_R\bar{t}_L)}{N(t_L\bar{t}_L + t_R\bar{t}_R) + N(t_L\bar{t}_R + t_R\bar{t}_L)}\ , \tag{8.6}$$

where $N_{||}$ and N_X give the number of events with parallel and anti-parallel top quark spins, respectively. Two angle combinations are considered: θ_l versus θ_b and θ_l versus $\theta_{q(lower\ energy)}$; in the following description these two combinations are denoted as $b-t\,l-t$ and $q-t\,l-t$.

8.3.2 Simulation of $t\bar{t}$ with spin correlation

A $t\bar{t}$ sample of $3.1 \cdot 10^6$ events containing $9.1 \cdot 10^5$ semi-leptonic signal events was generated with PYTHIA [24] and reconstructed using ORCA. As PYTHIA does not include spin correlations the events are weighted according to Formula 8.5 with $\mathcal{A} = 0.32$ [44] and appropriate values of κ. Then, this data sample is subdivided into two sub-samples: one is regarded as the "reference" sub-sample (1.61M events), used for determination of the selection efficiency and backgrounds. The other is regarded as the "analysis" sub-sample (1.50M events), used for the measurement of $\mathcal{A}$. This sample provides 436K signal events. The double differential angular distributions obtained from the "analysis" sample are presented in Figure 8.11.

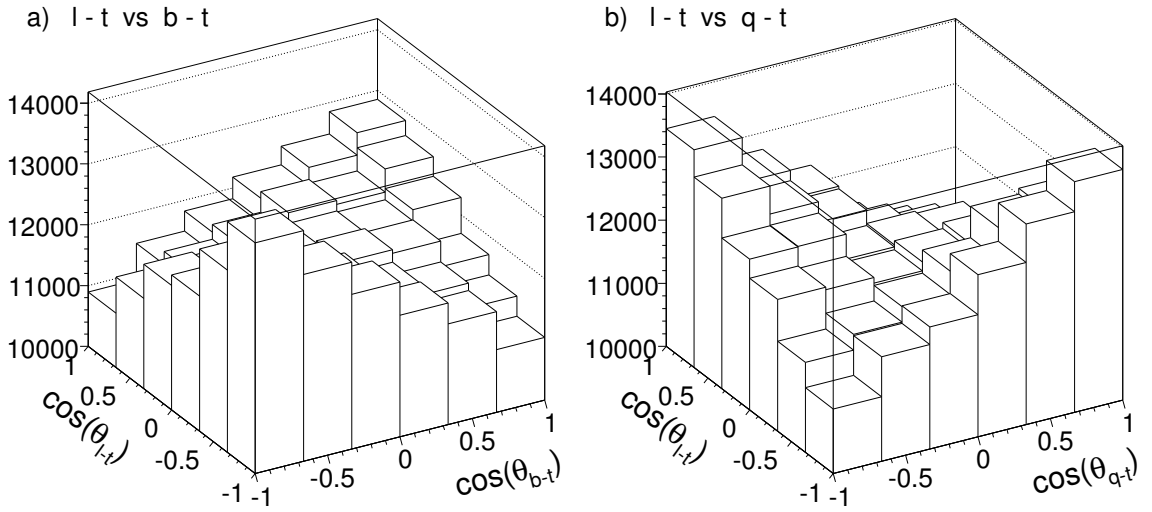

Figure 8.11: Double differential angular distributions obtained from the "analysis" sample, see text.

The distributions in Figure 8.11 are fitted according to the Formula (8.5). The results are $\mathcal{A}_{b-t\,l-t} = 0.321 \pm 0.011\,(\text{stat.})$ and $\mathcal{A}_{q-t\,l-t} = 0.319 \pm 0.009\,(\text{stat.})$ which are statistically compatible with the input value of $\mathcal{A} = 0.32$.

8.3.3 Online and offline event selection

The Level 1 and High Level triggers select events with a single isolated electron or muon; the trigger efficiency is 55%.

The following requirements are applied in the offline selection: missing transverse energy $E_{\mathrm{T}}^{\mathrm{miss}} > 20\,\mathrm{GeV}$; at least one isolated lepton with $|\eta| < 2.5$, electron with $p_{\mathrm{T}} > 27\,\mathrm{GeV/c}$ or muon with $p_{\mathrm{T}} > 20\,\mathrm{GeV/c}$; at least four jets with $p_{\mathrm{T}} > 30\,\mathrm{GeV/c}$ and $|\eta| < 2.5$. Jets are reconstructed with a cone algorithm with $\Delta R = 0.5$. At least two jets must be b-jets where the tagging efficiency is 66% for b quarks in $t\bar{t}$ events. This selection results in an overall efficiency of 12%.

The reconstruction of two top quarks includes the following requirements: Two jets that are not b-tagged and have an invariant mass in the range $50 - 135\,\mathrm{GeV/c^2}$, consistent with the W mass, are found. A b-tag jet which combined with the above reconstructed W gives an invariant mass in the range $130 - 250\,\mathrm{GeV/c^2}$, consistent with the t mass. In addition to the top quark reconstructed above, another top quark is required based on the other b-tag jet plus lepton and missing energy combination. The neutrino components are determined by fitting the missing energy components, constrained with W and t quark masses. The azimuthal angle between the two top quarks is required to be greater than 2 rad. This selection results in an overall efficiency of 5% (Table 8.15).

A measure of the selection quality can be obtained by comparing the generated and reconstructed momentum directions expressed in terms of the cosine of the angles defined above. Figure 8.12 presents the differences between the generated and reconstructed cosines of the $b-l\,l-t$ and $q-l\,l-t$ systems. Quantifying this selection quality Q as the ratio of the number of events in the four central bins to all bins, one obtains: $Q_{b-t\,l-t} = 52\%$ and $Q_{q-t\,l-t} = 45\%$.

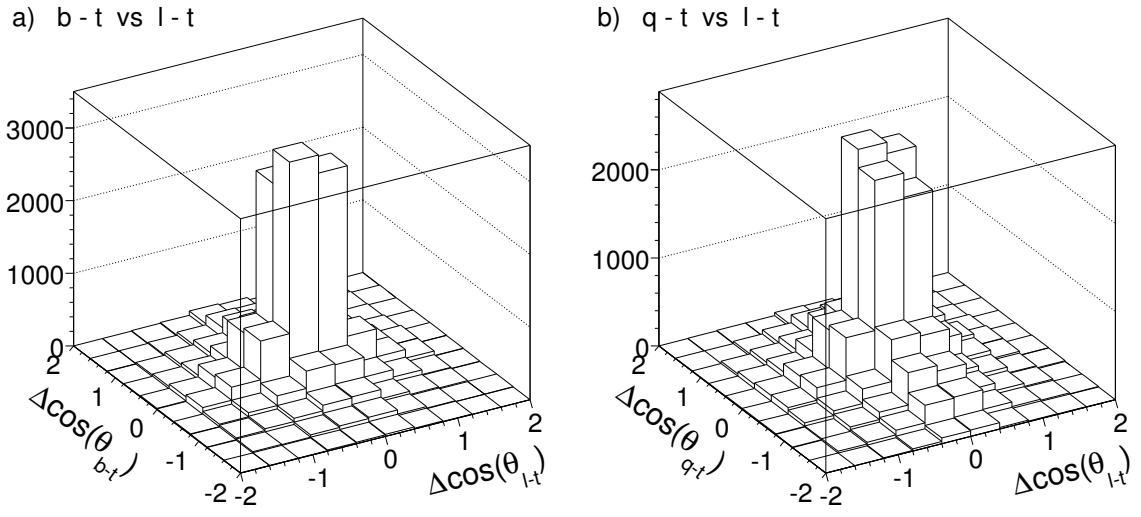

Figure 8.12: Selection quality: Difference between the generated and reconstructed cosine of the analysis angles in the $b - l\,l - t$ and $q - l\,l - t$ systems.

The signal-to-background ratio is 4.5. The main background, detailed in Table 8.15, is $t\bar{t}$ production with decays different from those treated as the signal. It amounts to 88% of the total background and is used to model the shape of the total background.

Table 8.15: The physics processes considered for signal and background. The number of selected events for the non-$t\bar{t}$ processes are scaled to the same $t\bar{t}$ sample luminosity.

Process	Simulated events	σ(pb)	Efficiency	Selected events
$t\bar{t}$ (signal)	436K	246	$5.0 \cdot 10^{-2}$	21589
$t\bar{t}$ (background)	1.07M	584	$4.0 \cdot 10^{-3}$	4236
$WW + \text{jets}$	310K	188	$4.5 \cdot 10^{-5}$	15
$W + \text{jets}$ ($\hat{p}_T = 20 - 400\,\text{GeV/c}$)	2.06M	43K	$3.4 \cdot 10^{-6}$	260
Wbt semi-leptonic decay	328K	63.1	$1.3 \cdot 10^{-3}$	144

8.3.4 Estimation of correlation coefficient

In order to correct for the selection efficiency, an efficiency (6×6) matrix is determined by taking the ratio of the reconstructed double differential angular distribution to the generated one, using the "reference" sample. The final double differential angular distribution is obtained by subtracting, bin-by-bin, the background obtained from the "reference" sample from the total sample of signal plus background obtained from the "analysis" sample. The resulting distributions are corrected for the selection efficiency, Figure 8.13, and fitted using Formula 8.5.

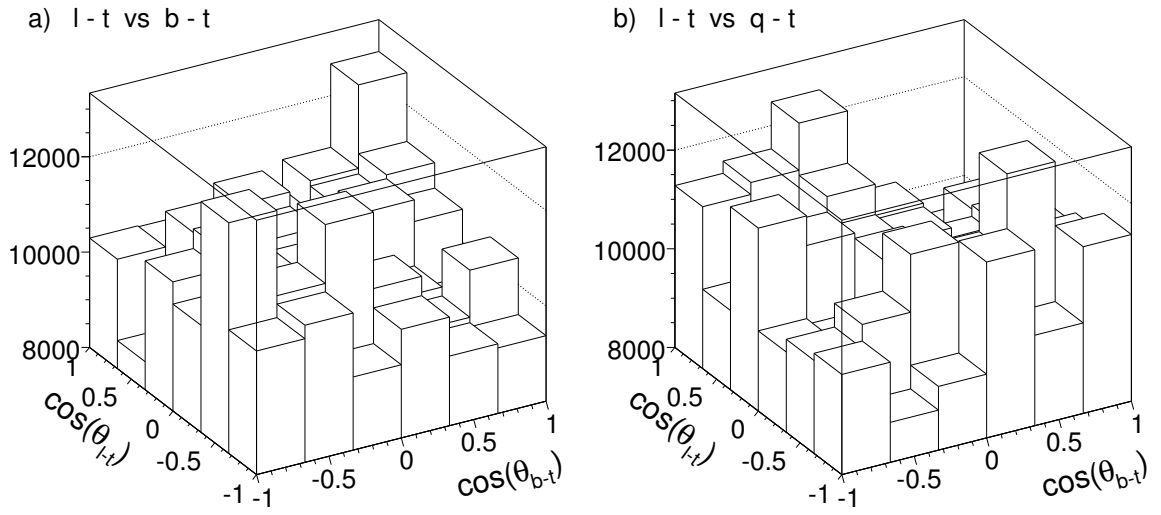

Figure 8.13: Background-subtracted and efficiency-corrected double-differential distribution of the cosine of the analysis angles in the $b - l\,l - t$ and $q - l\,l - t$ systems.

The correlation coefficients obtained from the fit are:

$$\mathcal{A}_{b-t\,l-t} = 0.375 \pm 0.100\,(\text{stat.})\,,$$
$$\mathcal{A}_{q-t\,l-t} = 0.346 \pm 0.079\,(\text{stat.})\,.$$

These results agree, within statistical uncertainties, with those obtained from the generated events of Figure 8.11.

The following sources of systematic uncertainties have been evaluated. The choice of the Parton Distribution Function in modelling $t\bar{t}$ production affects the number of $t\bar{t}$ events produced via gluon fusion and that via quark-anti-quark annihilation. The relative variation in $\mathcal{A}$, determined using TOPREX with different PDFs (CTEQ6M, MRST2003), is found to be 4%.

The mass of the top quark affects the result of the kinematic fit and the selection. The nominal $m_t = 175\,\text{GeV/c}^2$ is varied by $\pm 5\,\text{GeV/c}^2$ [54] using TOPREX. The variation in $\mathcal{A}$ is found to be negligible.

The uncertainty on the $t\bar{t}$ cross section affects the shape of the final angular distribution after background subtraction; varying $\sigma(t\bar{t})$ by 10% results in 1% relative variation in correlation coefficients.

The uncertainty due to b-tagging efficiency is evaluated by varying the b-identification discriminant cut. The corresponding relative variation in $\mathcal{A}_{b-t\,l-t}$ is -20%, and in $\mathcal{A}_{q-t\,l-t}$ it is $+6.5\%/-8.3\%$.

The jet energy scale uncertainty is evaluated by varying the jet P_T. The relative variations in $\mathcal{A}_{b-t\,l-t}$ and $\mathcal{A}_{q-t\,l-t}$ are found to be +7.7%/-14%.

Uncertainties in the initial and final state radiation, quark fragmentation, underlying event and pile up rate could result in an underestimation of the number of non-$t\bar{t}$ jets (not originating from top decays). This possible underestimation of jet multiplicity is estimated to be 8%. To estimate the corresponding uncertainty in $\mathcal{A}$, 10% additional jets per event are generated while processing the data sample. These jets are simulated randomly according to the η and p_{T} distributions of non-$t\bar{t}$ jets, obtained from the $t\bar{t}$ Monte Carlo. The relative variations in $\mathcal{A}_{b-t\,l-t}$ and $\mathcal{A}_{q-t\,l-t}$ are found to be -6.3% and -5.3%, respectively.

Summing up the systematic uncertainties and using the statistical uncertainties estimated for $10\,\text{fb}^{-1}$ of integrated luminosity, the results are:

$$\mathcal{A}_{b-t\,l-t} = 0.375 \pm 0.027\,(\text{stat.})^{+0.055}_{-0.096}\,(\text{syst.})\,,$$
$$\mathcal{A}_{q-t\,l-t} = 0.346 \pm 0.021\,(\text{stat.})^{+0.026}_{-0.055}\,(\text{syst.})\,.$$

In summary, the correlation coefficient of top quark spins in $t\bar{t}$ production is measured with a total relative uncertainty (dominated by systematic uncertainties) of 27% for $\mathcal{A}_{b-t\,l-t}$ and of 17% for $\mathcal{A}_{q-t\,l-t}$.

8.4 Single top quark production

8.4.1 Introduction

The single top production cross section at the LHC is known at NLO level for the tree production mechanisms (see Fig. 8.14, which are classified by the virtuality of the W-boson involved as: t-channel ($q^2_W < 0$), s-channel ($q^2_W > 0$), and associated tW production ($q^2_W = M^2_W$) [306–308]. In all cases, the most dangerous background comes from $t\bar{t}$ process. Other dangerous backgrounds are multi-jet QCD and W+jets events, but such background is reduced substantially by considering only leptonic decays of the $W^{\pm}$-bosons from top-quark decays.

All results presented in this Section were done for $10/\,\text{fb}^{-1}$ of integrated luminosity.

8.4.1.1 Details on the signal and background simulation

Two generators, SINGLETOP [309] (based on the COMPHEP package [43]) and TOPREX [44] were used to generate events for all three single-top production processes. The background processes, namely, $Wb\bar{b}$, $Wb\bar{b}+j$, and $W+2j$ were generated with COMPHEP, TOPREX,

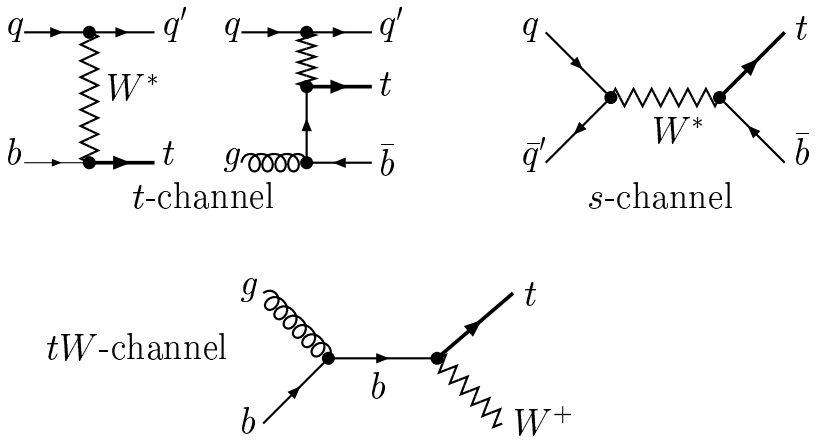

Figure 8.14: Feynman diagrams for the three channels of single top production.

MADGRAPH [80], and ALPGEN [160] programs as indicated in the Table 8.16. The hard process events containing all needed information were passed to PYTHIA 6.227 [24] for showering, hadronisation and decays of unstable particles. The $t\bar{t}$ and W + jets background events were generated with the same PYTHIA version. All simulations were done with $M_t = 175\,\text{GeV/c}^2$ and $M_b = 4.7 - 4.8\,\text{GeV/c}^2$, proper considerations of the spin correlations, and the finite W-boson and t-quark widths. The list of the signal and background process cross sections as well as generators used are given in the Table 8.16. Both the full simulation chain (OSCAR [8] and ORCA [10]) and a fast simulation (FAMOS [11]) were used.

Table 8.16: Cross section values (including branching ratio and kinematic cuts) and generators for the signal and background processes (here $\ell = e, \mu, \tau$). Different generator-level cuts are applied.

Process	$\sigma\times$BR, pb	generator	Process	$\sigma\times$BR, pb	generator
t-ch. ($W \to \mu\nu$)	18 (NLO)	SINGLETOP	$Wb\bar{b}$ ($W \to \ell\nu$)	100 (LO)	TOPREX
t-ch. ($W \to \ell\nu$)	81.7 (NLO)	TOPREX	$Wb\bar{b}$ + jets ($W \to \mu$)	32.4 (LO)	MADGRAPH
s-ch. ($W \to \ell\nu$)	3.3 (NLO)	TOPREX	$W + 2j$ ($W \to \mu\nu$)	987 (LO)	COMPHEP
tW (2 $W \to \ell\nu$)	6.7 (NLO)	TOPREX	$W + 2j$ ($W \to \ell\nu$)	2500 (LO)	ALPGEN
tW (1 $W \to \ell\nu$)	33.3 (NLO)	TOPREX	$Z/\gamma^*(\to \mu^+\mu^-)b\bar{b}$	116 (LO)	COMPHEP
$t\bar{t}$ (inclusive)	833 (NLO)	PYTHIA			

8.4.1.2 Reconstruction algorithms and triggers

Muons are reconstructed by using the standard algorithm combining tracker and muon chamber information as described in [310]; tracker and calorimeter isolation cuts are applied as described in [311]. The electrons are reconstructed by the standard algorithm combining tracker and ECAL information, see [312]. The jets are reconstructed by the Iterative Cone algorithm with the cone size of 0.5, see [313]; for the calibration both the Monte Carlo (in the t-channel analysis) and the $\gamma + jets$ (in the tW- and s-channel) methods are used, see [314]. For b-tagging a probability algorithm based on the impact parameter of the tracks is used, as described in [315].

The **transverse missing energy** is reconstructed as follows:

$$\vec{E}_{\mathrm{T}}^{\mathrm{miss}} = -\left(\sum \vec{P}_T^{\mu} + \sum \vec{E}_T^{tower} + \sum(\vec{E}_{T,jet}^{calib}) - \sum(\vec{E}_{T,jet}^{raw})\right) \tag{8.7}$$

where E_T^{tower} is the sum of transverse energy of towers, $E_{T,jet}^{calib}$ ($E_{T,jet}^{raw}$) is the transverse energy of calibrated (uncalibrated) jets. For the final states with one isolated lepton the neutrino ($E_{\mathrm{T}}^{\mathrm{miss}}$) longitudinal component, $P_{z,\nu}$, is extracted from the quadratic equation:

$$M_W^2 = 2\left(E_\mu\sqrt{P_{z,\nu}^2 + (E_{\mathrm{T}}^{\mathrm{miss}})^2} - \vec{P}_{T,\mu}\cdot\vec{E}_{\mathrm{T}}^{\mathrm{miss}} - P_{z,\mu}P_{z,\nu}\right) \tag{8.8}$$

This equation has two solutions:

$$P_{z,\nu}^{(1,2)} = \frac{AP_{z,\mu} \pm \sqrt{\Delta}}{P_{T,\mu}^2}, \quad \text{where } A = \frac{M_W^2}{2} + \vec{P}_{T,\mu}\cdot\vec{E}_{\mathrm{T}}^{\mathrm{miss}}, \ \Delta = E_\mu^2(A^2 - (E_{\mathrm{T}}^{\mathrm{miss}})^2 P_{T,\mu}^2) \tag{8.9}$$

Among the two solutions of Eq. (8.8) the minimal value of $|P_{z,\nu}|$ is used for W-boson momentum reconstruction.

About 30% of the events have negative Δ values due to the finite detector resolution and to the presence of extra missing energy. In this case for t-channel analysis the parameter M_W in Eq. (8.9) is increased until Δ becomes zero. Using this value of M_W, $P_{z,\nu}$ is calculated from Eq. (8.9). For the tW and s-channels analyses, only the real part of $P_{z,\nu}$ is used for further analysis.

The **transverse mass of the W-boson** is defined as

$$M_T^W = \sqrt{2(P_{T,\mu}E_{\mathrm{T}}^{\mathrm{miss}} - \vec{P}_{T,\mu}\cdot\vec{E}_{\mathrm{T}}^{\mathrm{miss}})}. \tag{8.10}$$

The **sum of the transverse momentum vectors** of all reconstructed objects

$$\vec{\Sigma}_T \equiv \vec{P}_{T,\ell} + \vec{E}_{\mathrm{T}}^{\mathrm{miss}} + \sum \vec{E}_{T,jet}, \tag{8.11}$$

is found to be very effective for signal/background separation.

The **"jet charge"** (Q_j) is defined as the sum of the charges of the tracks inside the jet cone, weighted over the projections of the track momenta along the jet axis.

The **lepton isolation** criterion used is to sum the p_{T} of all the tracks in a cone of $\Delta R < 0.2$ around the lepton track, and to reject the event if this sum is greater than 5% of the lepton p_{T}.

The present study is based on leptonic decay channels ($e\nu_e$ or $\mu\nu_\mu$) of the W-boson. The signal is triggered by the trigger on leptons. The HLT p_{T} thresholds from the CMS DAQ-TDR [75] are assumed: 19 GeV/c (29 GeV/c) for the single muon (electron); with $|\eta_\mu| \leq 2.1$ and $|\eta_e| \leq 2.4$.

8.4.1.3 The contribution from multi-jet backgrounds

A special treatment is required for QCD events with jets, due to the huge cross section. The currently available samples have very small statistics and typically no events remain after the application of pre-selection cuts. Therefore, in order to estimate the impact of the QCD-background the cuts are applied separately, assuming they are uncorrelated.

For t-channel study these cuts are: (a) one isolated muon ($p_{\rm T} > 19\,{\rm GeV/c}$); (b) $E_{\rm T}^{\rm miss} > 40\,{\rm GeV}$ and only two jets; one B-jet and one light forward jet. It was found a satisfactory suppression of the multi-jet events as compared to other background process ($N_{\rm QCD}/N_{\rm bckg} = 6924/(8.9 \times 10^4) = 0.078$ (see [316]) and the QCD-background was not considered in the analysis of the t- and s-channel single top production.

More detailed investigation of this problem was done for tW-channel [317]. The selection cuts are arranged into cut groups whose efficiencies are estimated with the Monte Carlo samples. The product of efficiencies is an indicator of the total efficiency.

Three cut groups are used in the dileptonic channel: lepton, $E_{\rm T}^{\rm miss}$, jet. The same procedure is applied on signal sample to find the ratio of total efficiency to the product of efficiencies. The ratio is used to correct the product of efficiencies found in multi-jet sample and the result is 5.6 events. Four cut groups are used in the semi-leptonic channel: jets, leptons, kinematics and finally signal region and b tagging. The b tagging requirement is taken out from jets group to have reasonable statistics for the efficiency measurement. By comparing the product of efficiencies with total efficiency of applying cut groups in series, the cut groups are found to be anti-correlated which would result in an over-estimate of the yield. The result of 508 events is kept to be conservative [317].

8.4.1.4 Systematic uncertainties

The following sources of systematic uncertainty are common for all three channels: (i) the **theoretical errors** to the total rates of the signal is $\Delta_{\rm th} \approx 4\%$, rising to 10% for tW. The uncertainties in the background events are assumed to be: 5% for $t\bar{t}$ [45], 17% for $Wb\bar{b}j$, 7% for $W+{\rm jets}$, 5% for Wjj [318], and 5% for $Wb\bar{b}$. (ii) the **jet energy scale (JES) uncertainty:** using a calibration method based on $t\bar{t}$ events [319], the JES uncertainty after $10\,{\rm fb}^{-1}$ integrated luminosity is expected to be $\pm 5\%$ ($\pm 2.5\%$) for jets with $p_{\rm T}$ ≈20 GeV/c ($p_{\rm T} > 50\,{\rm GeV/c}$). In the region between 20 and 50 GeV/c a linear dependence is assumed. (iii) **b-tagging identification uncertainty:** of $\pm 4\%$ on the overall selection efficiencies is expected on the b-tagging efficiencies [156]. (iv) the **luminosity uncertainty**, expected to be 5% [320].

8.4.2 Selection and cross section - t-channel

The final state in t-channel includes one isolated muon, missing energy (neutrino), one or two jets from b-quarks ($B_{\rm jet}$), and one "forward" hadronic jet. A specific feature of single top events is production of a light jet in the forward/backward direction (see Figs. 8.15) providing an additional possibility for background suppression. The additional b-quark is produced with small transverse momentum, making the reconstruction of the associated low-p_T jet and its b-tagging very difficult. Therefore, in t-channel analysis [316] it is required to have only two hadronic jets in the final state. In this case, the most important background contribution arises from $t\bar{t}$ production and from $W^{\pm}$-boson production in association with heavy quarks ($Wb\bar{b}$+jet) or light quark jets ($W + jets$).

8.4.2.1 Analysis of the fully simulated events

The selection requires the presence of only one isolated muon with $p_{\rm T} > 19\,{\rm GeV/c}$ and $|\eta_\mu| < 2.1$ (HLT selection). Then, it is required: (i) $E_{\rm T}^{\rm miss} > 40\,{\rm GeV}$; and (ii) at least two hadronic uncalibrated jets, with $p_{\rm T} > 20\,{\rm GeV/c}$. For further analysis the following additional requirements are: at least one of the selected jets should have the b-tag: the second (light) jet should be in the forward region; only two jets (calibrated) with $p_{\rm T}^{\rm calib} \geq 35\,{\rm GeV}$ and no other

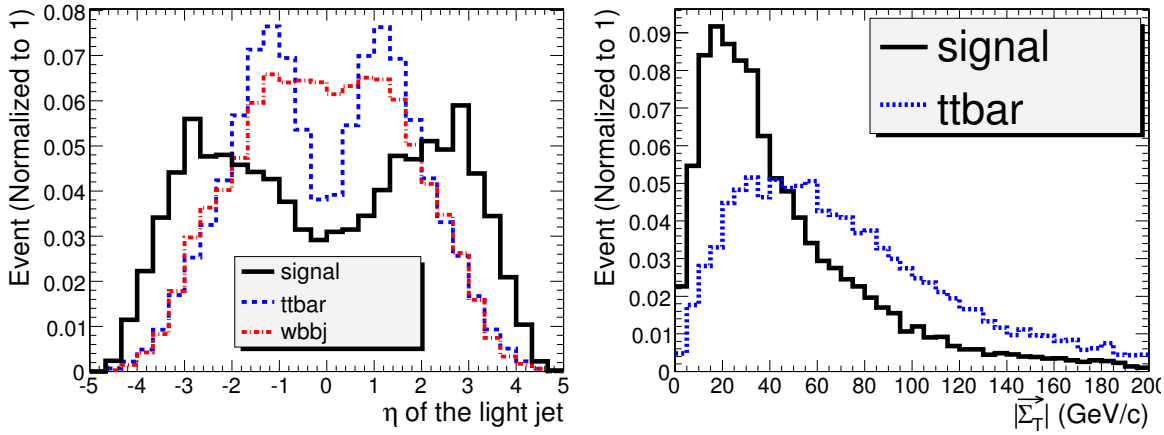

Figure 8.15: The distributions of pseudorapidity (η) of the light jet (left), and of $|\vec{\Sigma}_T|$ (right).

hadronic jets with $p_{\mathrm{T}}^{\mathrm{calib}} \geq 35\,\mathrm{GeV/c}$ (jet veto). The GARCON program [62] is used for the final optimisations of the cuts. The signal-over-background ratio times significance is chosen as an optimisation criterion. Finally, the optimal cut values found are:

- muon: $p_{\mathrm{T}}(\mu) > 19.0\,\mathrm{GeV/c}$ and $|\eta_{(\mu)}| < 2.1$ and $E_{\mathrm{T}}^{\mathrm{miss}} > 40.0\,\mathrm{GeV}$;
- b-jet: $p_{\mathrm{T}} > 35.0\,\mathrm{GeV/c}$, $|\eta| < 2.5$ and Discriminator > 2.4;
- the light forward: $p_{\mathrm{T}} > 40.0\,\mathrm{GeV/c}$ and $|\eta| > 2.5$;
- $|\vec{\Sigma}_T|$ cut window: (0.0, 43.5) GeV; $50 < M_T^W < 120\,\mathrm{GeV/c^2}$
- the reconstructed top mass window: $110\,\mathrm{GeV/c^2} < M_{\mathrm{rec}}(bW) < 210\,\mathrm{GeV/c^2}$

Table 8.17: Number of events (t-channel) and cumulative efficiencies for each cut used in the analysis of t-channel single top production. The symbol "$p_{TB} \times p_{Tj} \times E_{\mathrm{T}}^{\mathrm{miss}}$" means: $p_{TB} > 35\,\mathrm{GeV/c}$, $p_{Tj} > 40\,\mathrm{GeV/c}$, $|\eta_j| > 2.5$, $E_{\mathrm{T}}^{\mathrm{miss}} > 40\,\mathrm{GeV}$.

	signal	$t\bar{t}$	$Wb\bar{b}j$	Wj	Wjj
N(events) at $10\,\mathrm{fb}^{-1}$	1.8×10^5	8.33×10^6	3.24×10^5	9.7×10^7	9.9×10^5
isolated muon	0.73	0.14	0.52	0.16	0.81
$p_{TB} \times p_{Tj} \times E_{\mathrm{T}}^{\mathrm{miss}}$	0.036	6.4×10^{-3}	3.4×10^{-3}	9×10^{-6}	3×10^{-3}
veto on 3^{rd} jet	0.021	5.8×10^{-4}	1.6×10^{-3}	4×10^{-6}	1.1×10^{-3}
$0.0 < \Sigma_T < 43.5\,\mathrm{GeV}$	0.018	4.1×10^{-4}	1.2×10^{-3}	4×10^{-6}	6.8×10^{-4}
$50 < M_T^{W*} < 120$	0.015	2.2×10^{-4}	9.6×10^{-4}	1×10^{-6}	5.4×10^{-4}
$110 < M_{\mathrm{rec}}(bW)^* < 210$	0.013	1.4×10^{-4}	5.8×10^{-4}	0	4.1×10^{-4}
Number of events	2389	1188	195	0	402

* in $\mathrm{GeV/c^2}$

The efficiencies of these cuts and the resulting number of events are given in the Table 8.17. The resulting signal-to-background ratio and the significance are: $N_S/N_B = 1.34$ and $S_{stat} = N_S/\sqrt{N_S + N_B} = 37.0$. The final distribution of the reconstructed top mass is shown in Fig. 8.16. The cuts provide a satisfactory background suppression.

The systematic uncertainties (see Section 8.4.1.4) evaluated for $10\,\mathrm{fb}^{-1}$ are given in Table 8.18. In summary, the statistical error is 2.7%, the total systematic error excluding the 5% luminosity uncertainty is 8%, resulting in a total error of 10%.

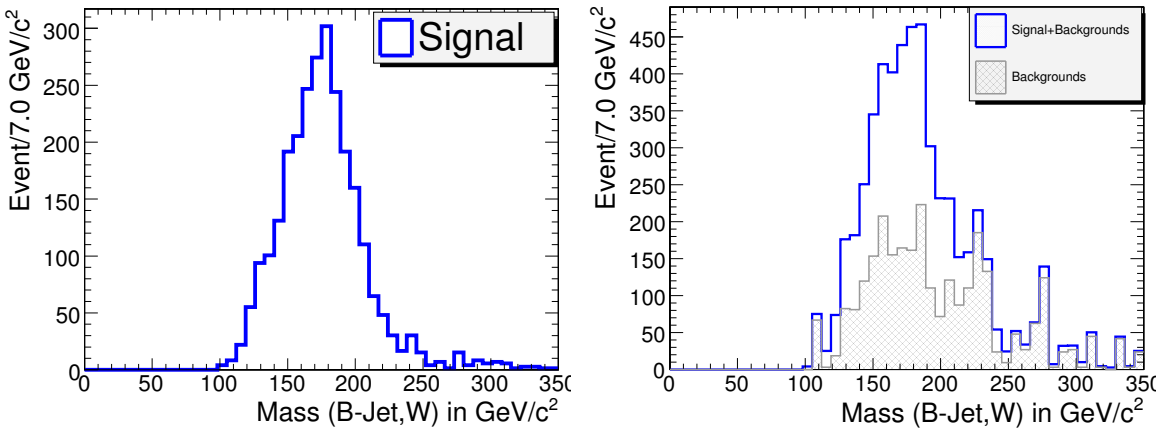

Figure 8.16: The distribution on the reconstructed top mass, for signal only (left) and with background included (right).

Table 8.18: Number of selected events (t-channel) at $10\,\text{fb}^{-1}$ with uncertainties due to different sources. ΔN_{syst} represents the theoretical, JES and b-tagging uncertainties. ΔN_{stat} is expected statistical uncertainty.

sample	selected	ΔN_{th}	JES	$\Delta N_{\text{b-tag}}$	ΔN_{syst}	ΔN_{stat}
t-channel	2389	96	71	96	153	49
$t\bar{t}$	1188	59	73	48	105	34
$Wb\bar{b}j$	195	33	6	8	35	14
Wjj	402	20	0	16	26	20

8.4.3 Selection and cross section - tW-channel

The $pp \to tW$ process contains two W-bosons and a b-quark in the final state. In this study only leptonic decays of the W's are considered. The nominal final states are $\ell^+\ell^- E_{\text{T}}^{\text{miss}} b$ and $\ell^\pm E_{\text{T}}^{\text{miss}} b\text{jj}$ for the dileptonic and semi-leptonic modes, respectively. The dominant background arises from $t\bar{t}$ production. Other backgrounds are t- and s-channel single top production, $Wb\bar{b}$, $W + \text{jets}$, $WW + \text{jets}$, and to a lesser extent QCD multi-jet background.

8.4.3.1 Jet quality requirements and extra jet reduction

The most significant difference between tW events and $t\bar{t}$ events is the number of jets in the final state. However, most of the time there are also additional jets due to the underlying event, pile-up or calorimeter noise. These "extra jets" were identified and excluded from the counting by consideration of five jet quality variables (see [317]). It was found that the most discriminating variables are E_{T}^{max} (the maximum tower E_{T} in a cone of 0.5) and N_{track} (the number of associated tracks). A Fisher discriminant [321] (F) is constructed from the jet quality variables to separate real jets from extra jets. Each jet is classified value F into one of three categories: good ($F < -0.5$), loose ($|F| < 0.5$) and bad ($F \geq 0.5$) jets. This method yields 84.3% efficiency on true jets and rejects 86.9% of extra jets. Only "good" jets and "loose" jets are used in pre-selection and event reconstruction. The jet multiplicity after the extra jet reduction in semi-leptonic channels reveals that the number of good jets peaks at the 2 and 3 jet bins for signal events, and at the 3 and 4 jet bins for $t\bar{t}$ backgrounds.

8.4.3.2 Event selection and reconstruction

The kinematic cuts used for this study are presented in Table 8.19 and Table 8.20. For the semi-leptonic channel, two non-b-like jets with $m_{jj} < 115\,\text{GeV/c}^2$ are used for reconstruction of the W-boson (that decays hadronically). In events with a 4th jet that survives jet veto cuts, it is required that the invariant mass of the 4th jet with any of the selected non-b-like jets must be outside a window of $M_W \pm 20\,\text{GeV/c}^2$. For the leptonic decays of the W-boson it is required that $M_T^W < 120\,\text{GeV/c}^2$.

Table 8.19: Kinematic cuts used in the dileptonic channel. The final electron and muon should have the opposite charges.

Leptons	**Jets**
$\|\eta(e)\| < 2.4$, $\|\eta(\mu)\| < 2.1$ $p_\text{T}(e,\mu) > 20\,\text{GeV/c}$ no other lepton with $p_\text{T} > 5\,\text{GeV/c}$	leading jet: $\|\eta\| < 2.4, p_\text{T} > 60\,\text{GeV/c}$, disc > 0 at most one extra jet No other jets with $p_\text{T} > 20\,\text{GeV/c}$
Missing E_T: $E_\text{T}^\text{miss} > 20\,\text{GeV}$	

Table 8.20: Kinematic cuts used in the semi-leptonic channel. The presence of a good fourth jet would veto the whole event.

Leptons
$p_\text{T}(e) > 30\,\text{GeV/c}$, $p_\text{T}(\mu) > 20\,\text{GeV/c}$, $\|\eta(e)\| < 2.4$, $\|\eta(\mu)\| < 2.1$ no other lepton $p_\text{T} > 10\,\text{GeV/c}$
Jets (after removing all bad quality jets)
b-like jet: good quality, disc>2, $\|\eta\| < 2.5$, $p_\text{T} > 35\,\text{GeV/c}$ non-b-like jet: good quality, $\|\eta\| < 3.0$, disc<0 if $\|\eta\| < 2.5$, $p_\text{T} > 35\,\text{GeV/c}$ Jet counting: one b-like jet and 2 non-b-like jets Jet veto: no other "good" or "loose" jets with $p_\text{T} > 20\,\text{GeV/c}$ and $\|\eta\| < 3$
Missing E_T: $E_\text{T}^\text{miss} > 40\,\text{GeV}$

To find the correct pairing of b-jet and reconstructed W-boson (coming from top decay) the following variables were used: the p_T of (b, W) systems; the separation of the b-jet with each of the W in (η, ϕ) space; the "charges" of jets (see Section 8.4.1.2) and W-bosons (see Ref. [317] for details). A Fisher discriminant based on these variables is used for discriminating leptonic top events from hadronic top events. A cut of 0.56 is optimal in separating these 2 types of events, and 72% of the events are correctly paired.

To further enhance the signal to background ratio the following "global" cuts are applied:

- p_T of the reconstructed tW system: $|\vec{\Sigma}(t+W)| < 60\,\text{GeV/c}$.
- Scalar sum of transverse energies H_T: $H_T < 850\,\text{GeV}$.
- Reconstructed top quark mass: $110\,\text{GeV/c}^2 < m(t) < 230\,\text{GeV/c}^2$.
- p_T of the reconstructed top quark: $20\,\text{GeV/c} < p_\text{T}(t) < 200\,\text{GeV/c}$.

8.4.3.3 Efficiencies and expected yields

The efficiencies estimated with Monte Carlo samples are converted to the effective cross sections by multiplying the production cross sections of each process. The effective cross

sections, as well as the expected yields with $10\,\text{fb}^{-1}$ of data for all signal and background samples, are shown in Table 8.21 and 8.22. The signal to background ratio is found to be 0.37 for dileptonic channel and 0.18 for semi-leptonic channel.

Table 8.21: Summary of cross section times branching ratio times efficiencies at each stage of the analysis for the dileptonic channel. All values are in picobarns The last row is the expected number of events for $10\,\text{fb}^{-1}$. Multi-jet background has been estimated separately (see Section 8.4.1.3). When only a limit on the number of events is stated, this is due to MC statistics.

	tW dil.	$t\bar{t}$ dil.	$t\bar{t}$ oth.	WW dil.	WW oth.	t ch. lept.
Production	6.667	92.222	737.778	11.111	88.889	81.667
HLT	4.865	74.090	346.151	7.674	27.259	41.409
$2\,\ell$	1.944	25.150	21.012	2.574	0.226	2.309
Lepton p_{T}	0.675	7.919	0.703	0.543	0.012	0.098
≤ 1 extra jet	0.459	6.574	0.664	0.416	0.010	0.067
Jet p_{T}, η	0.307	5.234	0.556	0.339	0.004	0.033
≥ 1 b-jet	0.184	3.864	0.379	0.017	0.000	0.018
$E_{\text{T}}^{\text{miss}} > 20$	0.170	3.640	0.349	0.017	0.000	0.016
≤ 2 jet	0.150	2.734	0.221	0.015	0.000	0.012
Final select.	0.057	0.145	0.000	0.006	0.000	0.000
Expected events	567	1450	≤ 55	61	≤ 10	≤ 20

Table 8.22: Summary of cross section times branching ratio times efficiencies at each stage of the analysis for the semi-leptonic channel. All values are in picobarns. The last row is the expected number of events for $10\,\text{fb}^{-1}$.

	tW	$t\bar{t}$	t ch.	s ch.	Wbb	W2j	W3j	W4j	Multi-jet
Total cross section	60	833	245	10	300	7500	2166	522	9.73×10^{9}
HLT	18.9	263.9	39.5	1.52	34.0	1006	300	73	1.86×10^{5}
Presel. & isolation	9.05	179.4	12.0	0.54	2.15	52	35	12	1325
jet & lepton p_{T}, jet veto	1.28	18.5	1.31	0.046	0.061	0.60	4.9	1.0	4.23
b-tagging	0.669	6.13	0.476	0.013	0.016	0.10	0.99	0.26	0.85
kinematic cuts	0.223	0.999	0.047	0.002	0.003	0.017	0.101	0.008	0.105
Signal box cuts	0.170	0.771	0.035	0.001	0.001	0.013	0.054	0.008	0.051
Events in $10\,\text{fb}^{-1}$	1699	7709	351	14	10	130	539	80	508

8.4.3.4 The ratio method

The *ratio method* is developed to reduce systematic uncertainties related to the dominant $t\bar{t}$ background. We define a $t\bar{t}$-rich control region and use ratio of efficiencies to estimate the yield of $t\bar{t}$ in the signal region. The kinematics of tW and $t\bar{t}$ are similar so tW is present in the control region, therefore the ratio of efficiencies for tW is also used. The signal and

background yield is determined by the following equation:

$$S = \frac{R_{t\bar{t}}(N_s - N_s^o) - (N_c - N_c^o)}{R_{t\bar{t}} - R_{tW}}, \quad (8.12)$$

$$B = \frac{(N_c - N_c^o) - R_{tW}(N_s - N_s^o)}{R_{t\bar{t}} - R_{tW}} + N_s^o. \quad (8.13)$$

Here R_x is the ratio of efficiencies $R_x = \epsilon_x$(control region)/ϵ_x(signal region) for $x = t\bar{t}, tW$; N_s (N_c) is total number of events in the signal (control) region; N_s^o (N_c^o) is the estimated number of non-$t\bar{t}$ background events in the signal (control) region. With S measured with 2 regions and the ratio method, the cross section can be found by $S/\epsilon\mathcal{L}$.

For the ratio method to work it is important to find a control region with similar kinematics except with one more jet. It is expected that systematic uncertainties from PDF, JES and b tagging cancel to a large extent, while the luminosity uncertainty drops out for the $t\bar{t}$ background. The lepton selection and jet quality requirements in the control region are identical to the signal region. The differences are outlined below.

Dileptonic. A second jet is required with $p_{\mathrm{T}} = 20 - 80\,\mathrm{GeV/c}$, $|\eta| < 2.4$ and b-tagged (disc > 0). No other jets with $p_{\mathrm{T}} > 20\,\mathrm{GeV/c}$ are allowed. The background region is found to be filled by 97.9% dileptonic $t\bar{t}$, 0.4% other $t\bar{t}$ decays, 1.6% dileptonic tW, and 0.1% for leptonic t channel single top while WW+jets yield is negligible.

Semi-leptonic. It requires 2 jets with $p_{\mathrm{T}} > 30$, 2 more jets with $p_{\mathrm{T}} > 20$, and no bad jets with $p_{\mathrm{T}} > 20$. It is required that one of the 2 high-p_{T} jets is b-tagged (disc > 2), and that both low-p_{T} jets be not tagged (disc < 0). The $b - W$ pairing is done in the same way, with a 72% correct pairing. It is found that the $t\bar{t}$ purity in the control region is 93.9%. The non-$t\bar{t}$ events are mainly composed of W+jets (2.8%), tW (2.0%) and t-channel single top (1.2%). The ratio of efficiencies are found to be R_{tW} = 0.319 and $R_{t\bar{t}}$ = 3.31.

8.4.3.5 Systematic uncertainties

• **Theoretical uncertainties** The $t\bar{t}$ cross section does not show up in the ratio method. The effect is 0.8% for t-channel single top and 3.1% for W+jets. It is found to be negligible for other background.
• **Pileup amount** A difference of 30% between normal pileup and no pileup is used as an estimate of the systematic uncertainty, as was done in [200] for the dileptonic $t\bar{t}$ studies.
◇ *Dileptonic mode* The analysis is found to be rather sensitive to the pileup, as the relative shift of the "measured" cross section is $+20.4\%$ for no pileup, and -16.2% for double pileup, while is the difference between the check sample and the reference sample 4.6% (which has purely statistical origin). The value of 6.1% is used as the systematic uncertainty.
◇ *Semi-leptonic mode* The extracted cross section varies by $+35\%$ for no pileup and -63% for double pile-up so a systematic uncertainty of 10.3% is obtained. The results for both channels are shown in table 8.23.

The results from the ratio method were used in the significance calculation. In addition, the uncertainty on the background expectation, evaluated for dileptonic ($\Delta_B/B = \pm 9.6\%$) and semi-leptonic ($\Delta_B/B = +3.6\%/-4.4\%$), was taken into account. The resulting significance is 4.2 for the dileptonic channel and 5.1 for the semi-leptonic channel. Combining the two channels gives a total significance of 6.4.

Table 8.23: Summary of uncertainties of cross section measurement.

Source	Uncertainty	$\Delta\sigma/\sigma$ (dilept.)	$\Delta\sigma/\sigma$ (semi-lept.)
Statistical uncertainty	—	8.8%	7.5%
Integrated luminosity	5%	5.4%	7.8%
$t\bar{t}$ cross-section	9%	*negligible*	*negligible*
t-channel cross-section	5%	*negligible*	0.8%
W+jets cross-section	10%	*not applicable*	3.1%
WW+jets cross-section	10%	1%	*not applicable*
Jet energy scale	5%-2.5%	19.7 %	9.4%
b tagging efficiency	4% - 5%	8.7 %	3.6%
PDF	1σ	+4%/-6.0%	1.6%
Pileup	30%	6.1 %	10.3%
MC statistics	—	9.9%	15.2%
Total uncertainty		$\pm$23.9%(syst.) $\pm$ 9.9%(MC)	$\pm$16.8%(syst.) $\pm$15.2%(MC)

8.4.4 Selection and cross section - s-channel

The present analysis of the s-channel single top production is based on leptonic channels, i.e. the top is identified and reconstructed by its semi-leptonic decays into $\ell\nu b$ final states, with $\ell = e, \mu$. For this study, a fast simulation of the CMS detector with FAMOS was used, see [316, 317] for details.

The signal events are triggered by the single lepton triggers. Since this production mode suffers from low statistics, one could envisage the introduction of a combined trigger $e \times jet$, with threshold 19 GeV/c for the electron (in order to make the electronic sample more coherent with the muonic sample) and 45 GeV/c for the jet. This value has been chosen to be the same as the threshold for the τ-jet in the already existing $e \times \tau - jet$ trigger.

8.4.4.1 Pre-selection

The pre-selection criteria are as follows:

- The event has to fire at least one of the previously described triggers (including the proposed $e \times j$).
- The event must contain one isolated lepton (μ or e) with $p_{\mathrm{T}} \geq 19\,\mathrm{GeV/c}$ and $|\eta| \leq 2.1 (\leq 2.4)$ for muons (electrons) and no other lepton above $10\,\mathrm{GeV/c}$.
- Exactly two uncalibrated jets must have $p_{\mathrm{T}} \geq 30\,\mathrm{GeV/c}$ and $|\eta| \leq 2.5$ and no other jet has to be present with $p_{\mathrm{T}} \geq 20\,\mathrm{GeV/c}$.
- Both jets should have a positive b-tagging discriminator value.
- The event should have $E_{\mathrm{T}}^{\mathrm{miss}} > 30\,\mathrm{GeV}$.
- The transverse mass of the W-boson M_T^W should be less than $100\,\mathrm{GeV/c^2}$.

Details on the effect of the pre-selection cuts are given in Table 8.24. Note, that as in Section 8.4.2, the multi-jet QCD contribution is neglected.

Table 8.24: Efficiencies of the pre-selection cuts, with respect to the initial number of events. For all process (except of $t\bar{t}$) the final W decays into charged lepton ($\ell = e, \mu, \tau$) and neutrino. "HLT" includes the 1μ, $1e$ and $e \times j$ triggers. N_{ev} is the number of events surviving these cuts (the uncertainties are only those due to the limited Monte Carlo statistics).

Cut	s-ch.	t-ch.	$t\bar{t}$	$Wb\bar{b}$	Wt ($1\ W \to l\nu$)
"HLT"	$37.5 \pm 0.2\%$	$42.5 \pm 0.1\%$	$30.1 \pm 0.1\%$	$29.4 \pm 0.1\%$	$46.5 \pm 0.1\%$
Isolation	$33.7 \pm 0.2\%$	$39.0 \pm 0.1\%$	$21.7 \pm 0.1\%$	$28.2 \pm 0.1\%$	$42.3 \pm 0.1\%$
$E_{\mathrm{T}}^{\mathrm{miss}}$ cut	$27.3 \pm 0.2\%$	$31.9 \pm 0.1\%$	$17.4 \pm 0.1\%$	$22.6 \pm 0.1\%$	$34.4 \pm 0.1\%$
M_T^W cut	$23.2 \pm 0.2\%$	$26.3 \pm 0.1\%$	$13.6 \pm 0.1\%$	$18.4 \pm 0.1\%$	$29.2 \pm 0.1\%$
$N_j \geq 2j$	$11.9 \pm 0.1\%$	$11.5 \pm 0.1\%$	$11.9 \pm 0.1\%$	$0.88 \pm 0.03\%$	$18.5 \pm 0.1\%$
$N_j = 2j$	$8.9 \pm 0.1\%$	$8.2 \pm 0.1\%$	$1.84 \pm 0.04\%$	$0.76 \pm 0.03\%$	$7.09 \pm 0.05\%$
b-tag	$3.07 \pm 0.07\%$	$0.72 \pm 0.02\%$	$0.28 \pm 0.02\%$	$0.14 \pm 0.01\%$	$0.34 \pm 0.01\%$
N_{ev}	1010 ± 10	5880 ± 70	23300 ± 200	1400 ± 35	1150 ± 40

8.4.4.2 Genetic algorithm analysis

The following observables have been chosen in order to further discriminate between signal and background after pre-selection: (i) the jet b-tagging discriminants; (ii) the calibrated jet transverse momenta; (iii) the mass of the reconstructed top; (iv) $|\Sigma(t, \bar{b})|$; (v) the scalar sum of the transverse momenta of all the reconstructed objects. The reconstructed top quark is formed by the reconstructed W and one of the two b-jets, chosen according to the value of the "jet charge" (Q_j, see Section 8.4.1.2). Since in top decays the W and the original b quark have opposite sign of the charge, the jet with Q_j "most opposite" to the W is used for top reconstruction, leading to a probability of 67% to identify the correct pairing.

The cuts on these variables are optimised by means of the GARCON program [62]. The surviving events after these cuts are shown in cascade in Table 8.25. With this selection, after an integrated luminosity of 10 fb^{-1} one gets: $N_S/N_B \approx 0.13$.

Table 8.25: Final cuts and their efficiencies, with respect to the preselected samples, for the signal and the main backgrounds. For s- and t-channel and $Wb\bar{b}$ samples the final W-boson decays into lepton (e, μ, τ) and neutrino. $t\bar{t}$ samples includes all W-boson decay modes.

Cut	s-channel	t-channel	$t\bar{t}$	$Wb\bar{b}$
b-tag(j_1)> 0.4, b-tag(j_2)> 0.1	85%	75%	78%	85%
$p_{\mathrm{T}}(j_1) > 50\,\mathrm{GeV/c}$, $p_{\mathrm{T}}(j_2) > 50\,\mathrm{GeV/c}$	68%	53%	70%	37%
$120 < M(l\nu b) < 220\,\mathrm{GeV/c^2}$	52%	34%	46%	26%
$25 < p_{\mathrm{T}}(l\nu b) < 160\,\mathrm{GeV/c}$	48%	32%	43%	26%
$\Sigma_T < 20\,\mathrm{GeV/c}$	35%	15%	10.6%	12.5%
$H_T < 340\,\mathrm{GeV/c}$	27%	10.7%	5.4%	11.1%
number of surviving events	273 ± 4	630 ± 14	1260 ± 60	, 155 ± 12

8.4.4.3 Systematic uncertainties

In addition to systematics described in Section 8.4.1.4 the following sources of systematic uncertainty are considered:

• **Top mass.** The variation of m_t within $\pm 2\,\mathrm{GeV/c^2}$ around top mass $m_t = 175\,\mathrm{GeV/c^2}$ leads to the relative systematic error on the selection efficiency $\sigma_{\mathrm{syst}}^{m_t}$ =0.5% for the s-channel single top.

• **Parton Distribution Functions.** To extract the dependence on the PDF uncertainty, two different PDF sets were used: CTEQ61and CTEQ6M [12]. The result is $\sigma_{\rm syst}^{\rm PDF}$ =0.7%.
• **Initial/Final State Radiation modelling.** The model parameters were varied in the ranges $\Lambda_{\rm QCD}$=0.25±0.1 GeV and $Q^2_{\rm max}$ from 0.25 to 4 $\hat{s}$ (see [200]). The extreme values of the efficiencies are taken as systematic error: $\sigma_{\rm syst}^{\rm rad} = 0.5\%$.

Table 8.26: Number of selected events after 10 fb^{-1} and systematic uncertainties.

sample	selected	$\Delta\sigma$	JES	b-tag	M_{top}	PDF	ISR/FSR
S: s-channel	273	—	±3	±11	±1.5	±2	±1.5
B: t-channel	630	±25	±8	±25	—	—	—
B: $t\bar{t}$	1260	±63	±75	±50	—	—	—
B: $Wb\bar{b}$	155	±8	±7	±6	—	—	—

8.4.4.4 Background normalisation

The $t\bar{t}$ events in Table 8.26 are, in 41% of the cases, $t\bar{t} \to l^+\nu bl^-\bar{\nu}\bar{b}$ events with a lepton missed, and in the remain cases $t\bar{t} \to l^+\nu bq\bar{q}'\bar{b}$ events with two jets missed ($t\bar{t} \to q\bar{q}'bq\bar{q}'\bar{b}$ events give a negligible contribution). These two categories of events are very differently affected by the Jet Energy Scale variation. In general, any variation going in the direction of more jets gives a better rejection of the $t\bar{t} \to l^+\nu bq\bar{q}'\bar{b}$ component with respect to the signal, while the $t\bar{t} \to l^+\nu bl^-\bar{\nu}\bar{b}$ events, having two quarks, are affected almost in the same way as the signal.

• *$t\bar{t} \to \ell^\pm + X$ enriched control sample*
In this case the difference with respect to Sec. 8.4.4.1 is the request of three jets instead of two and only the muon channel is used. The selection efficiency for $t\bar{t} \to \ell^\pm$ events is found to be 1.08%. The ratio R_{c1} between the efficiencies in the main sample and in this control sample is $R_{c1} = 0.0149$, whose variations under JES and b-tagging efficiency systematic shifts are $\Delta R_{c1} = \pm 0.0015(JES) \pm 0.0003(b-tag)$.

• *$t\bar{t} \to \ell^+\ell^- + X$ enriched control sample*
This sample is obtained by the same selection as in Sec. 8.4.4.1, but two leptons with different flavours with the opposite sign are required. The selection efficiency for $t\bar{t} \to 2l$ events is found to be 0.822%. The ratio R_{c2} between the efficiencies in the main sample and in this control sample is $R_{c2} = 0.0681$, whose variations under JES and b-tagging efficiency systematic shifts are $\Delta R_{c2} = \pm 0.0010(JES) \pm 0.0004(b-tag)$.

8.4.4.5 Results

The number of the selected signal (N_S) and background (N_B) events and their estimated uncertainties are listed in Table 8.26. The cross section is extracted as

$$\sigma = \frac{N_{tot} - b^0 - R_{c1}(N_{c1} - b^0_{c1}) - R_{c2}(N_{c2} - b^0_{c2})}{\epsilon L}, \tag{8.14}$$

where b^0 is the sum of the non-top backgrounds in the main sample, N_{c1} and N_{c2} are the total events selected in the two control regions, and b^0_{c1} and b^0_{c2} are their contamination by non-top backgrounds, single top and other $t\bar{t}$ decays. The statistical error is evaluated to be 18%. The total systematic uncertainty is 31%, where the largest contribution arises from the effect of the JES uncertainty, on the $t\bar{t}$ single lepton background. The use of "Energy Flow" techniques, including the charged tracks information, is expected to significantly reduce this uncertainty. The total error, including also the 5% luminosity uncertainty, is 36%.

8.4.5 Conclusion

Selection strategies have been proposed for all the three single top production modes, and their effectiveness is shown, taking into account the expected statistics after 10 fb^{-1}. All analyses will be systematics dominated. For the s-channel and tW-associated cases, control samples have been proposed in order to constrain the dominant $t\bar{t}$ background.

The resulting signal-to-background ratio and the significance for the t-channel are: $N_S/N_B = 1.34$ and $S_{stat} = N_S/\sqrt{N_S + N_B} = 37.0$, with a statistical error of 2.7%, and a systematic error excluding the 5% luminosity uncertainty of 8%, resulting in a total error of 10%. For tW-channel we expect to reach the significance of 4.2 (5.1) for the dilepton (semi-leptonic) channel, increasing to 6.4 after combining the two channels. The total uncertainty is $\pm$23.9%(syst.) $\pm$9.9%(MC) for dilepton and $\pm$16.8%(syst.) $\pm$15.2%(MC) for semi-leptonic channels. The total systematic uncertainty for the s-channel is 31%. The total error, including also the 5% luminosity uncertainty, is 36%.

8.5 Search for flavour changing neutral currents in top decays

8.5.1 Introduction

The study of Flavour Changing Neutral Current (FCNC) interactions plays an important role in testing the Standard Model (SM) and probing new physics beyond it. The top quark is regarded to be more sensitive to new physics than other fermions, due to its mass close to the electroweak scale. Owing to the GIM mechanism of the SM, top quark FCNC interactions are absent at tree level and extremely small at loop level.

In recent years a lot of work has been done to explore the top quark FCNC couplings. On the theoretical side, various FCNC top quark decays and top-charm associated production at high energy colliders were extensively studied in the SM [322, 323], the Minimal Supersymmetric Standard Model (MSSM) [324–327] and other new physics models [328–332]. In models beyond the SM the top quark FCNC branching fractions may be significantly enhanced. Thus searching for top quark FCNC is a potentially powerful probe of new physics. The CDF and DØ collaborations have reported interesting bounds on the FCNC top quark decays [333–335]. The SM expectations for such top quark FCNC processes are far below the detectable level but the MSSM can enhance them by several orders of magnitude to make them potentially accessible at future collider experiments [336–338]. The theoretical branching ratios and the experimental limits are summarised in Table 8.27. Details of this analysis can be found in [339].

Table 8.27: Theoretical branching ratios of FCNC top quark decays in various models and experimental limits

Decay	SM	two-Higgs	SUSY with $\not{R}$	Exotic Quarks	Exper. Limits(95% CL)
$t \to gq$	5×10^{-11}	$\sim 10^{-5}$	$\sim 10^{-3}$	$\sim 5 \times 10^{-4}$	< 0.29 (CDF+TH)
$t \to \gamma q$	5×10^{-13}	$\sim 10^{-7}$	$\sim 10^{-5}$	$\sim 10^{-5}$	< 0.0059 (HERA)
$t \to Zq$	$\sim 10^{-13}$	$\sim 10^{-6}$	$\sim 10^{-4}$	$\sim 10^{-2}$	< 0.14 (LEP-2)

8.5.2 Signal and background generation

Both the $t \to \gamma q$ and the $t \to Z^0 q$ decay channels are investigated. The channel $t \to gq$ is not studied because of its very high background. The $t\bar{t}$ signal is generated with TOPREX [44], while PYTHIA [183] is used for modelling of quark and gluon hadronisation. The $t\bar{t}$ pair is generated through gluon-gluon and quark-anti-quark annihilation, with subsequent SM decay for one top ($t \to Wb$) and FCNC decay of the other. Only leptonic decay channels of Z and W bosons are studied, where the lepton could be either e or μ. Hadronic Z/W decays as well as decays to tau leptons are not considered because of the large QCD background. On generator level both top quarks are produced on-shell, with a mass of $m_t = 175\,\text{GeV/c}^2$, including the effects of spin-state correlations on final decay products (γq, $Z^0 q$, Wb). Both ISR and FSR are simulated with CTEQ5L PDFs. The generated events are passed through the full detector simulation and digitisation, taking into account low luminosity pile-up.

Several SM processes contributing as background are studied: $t\bar{t}$ production, single top quark production (t-channel), $ZW + \text{jets}$, $WW + \text{jets}$, $ZZ + \text{jets}$, $W + \text{jets}$, $Z + \text{jets}$, $Zb\bar{b}$ and QCD multi-jet production.

8.5.3 Selection strategies

The $t \to \gamma q$ channel is well identified by a high-energy isolated photon accompanying the FCNC top decay. One b-tagged jet and a light jet are also used to distinguish from the standard $t\bar{t}$ decays. For the FCNC $t \to \gamma q$ channel our main selection cuts are: (a) 'single electron or single muon' trigger criteria at Level-1 and HLT levels; (b) one isolated $e^{\pm}$ (with $p_T > 30\,\text{GeV/c}$) or $\mu^{\pm}$ (with $p_T > 20\,\text{GeV/c}$), and missing transverse energy $E_{\text{T}}^{\text{miss}} > 25\,\text{GeV}$, forming a transverse invariant mass $M_T(bW) < 120\,\text{GeV/c}^2$; (c) only one jet compatible with b-jet with $p_T > 40\,\text{GeV/c}$, that in combination with the W candidate gives an invariant mass in the range between $110\,\text{GeV/c}^2$ and $220\,\text{GeV/c}^2$; (d) one single isolated photon with $p_{\text{T}} > 50\,\text{GeV/c}$; (e) one light-jet (not compatible with b-jet) with $p_{\text{T}} > 50\,\text{GeV/c}$; (f) an invariant mass obtained from the combination of the photon and the light jet that lies in the range between $150\,\text{GeV/c}^2$ and $200\,\text{GeV/c}^2$; (g) the transverse momentum of the photon + light-jet system recoiling against the transverse momentum of the SM-decaying top quark satisfying $\cos\phi(t\bar{t}) < -0.95$.

The total efficiency for the signal is $\epsilon = 0.021 \pm 0.002$. Only the SM backgrounds $t\bar{t}$ and EW single top (t-channel) contribute to the accepted background, with 54 ± 7 background events accepted for a luminosity of $10\,\text{fb}^{-1}$. The uncertainties are statistical only.

Adopting a factorisation method, QCD background is proven to be not dangerous for the analysis: A set of independent cuts (hard jets, isolated hard lepton, isolated hard photon, b-tagging) is applied to both QCD and $t\bar{t}$ background and the efficiencies for single cuts are assumed to factorise. The b-tagging efficiency and the mistagging are 30% and 0.5%. The number of surviving QCD events for this pre-selection is found to be 42 for a luminosity of $10\,\text{fb}^{-1}$, and the efficiency on the $t\bar{t}$ sample amounts to 2.5%. Assuming that after these cuts the further efficiency for the QCD backgrounds and $t\bar{t}$ is the same, leads to expect $\simeq 1$ background events.

For the FCNC $t \to Z^0 q$ channel our main selection cuts are: (a) 'double electron or double muon' trigger criteria at Level-1 and HLT levels; (b) two isolated $e^{\pm}$ (each with $p_T > 20\,\text{GeV/c}$) or $\mu^{\pm}$(each with $p_T > 10\,\text{GeV/c}$), having an invariant mass $\pm 10\,\text{GeV/c}^2$ around the nominal Z^0 mass; (c) third lepton (e with $p_T > 20\,\text{GeV/c}$ or μ with $p_T > 15\,\text{GeV/c}$), which,

in combination with the missing transverse energy ($E_{\mathrm{T}}^{\mathrm{miss}} > 20\,\mathrm{GeV}$) have a transverse mass less than 120 GeV/c^2; (d) only one jet compatible with b jet with $p_T > 40\,\mathrm{GeV/c}$; (e) invariant mass of candidate W and b jet in the range [110-220] GeV/c^2; (f) one light-jet (not compatible with b jet) with $p_T > 30\,\mathrm{GeV/c}$ (g) an invariant mass obtained from the combination of the Z and the light jet that lies in the range between 110 GeV/c^2 and 220 GeV/c^2; (h) the transverse momentum of the Z + light-jet system recoiling against the transverse momentum of the SM-decaying top quark satisfying $\cos\phi(t\bar{t}) < 0$.

The total efficiency for the signal is $\epsilon = 0.041 \pm 0.002$. A total of 1 ± 1 background events are accepted for a luminosity of 10 fb^{-1}. The SM background $t\bar{t} \rightarrow (\nu lb)(\nu lb)$ is the only background that gives a significant contribution. The uncertainties are statistical only.

8.5.4 Sensitivity estimation

For the FCNC sensitivity estimation, it is assumed that new physics is observed when the signal significance is 5 at least. When dealing with a small number of background (B) events with respect to signal ones (S), an appropriate definition of significance is [49]:

$$S_{12} = 2\left(\sqrt{B+S} - \sqrt{B}\right) \tag{8.15}$$

S_{12} defines the probability (in number of sigmas) that a background with expected value B fluctuates above observed number of events $S + B$ with Poisson statistics. The number of signal events for the $t \rightarrow Zq$ and $t \rightarrow \gamma q$ channel can be expressed as:

$$\begin{aligned} S(t \rightarrow Zq) &= 2 \times BR(t \rightarrow Zq) \times Br\,(W \rightarrow l\nu) \times Br\,(Z \rightarrow ll) \times \sigma(t\bar{t}) \times L \times \epsilon(t \rightarrow Zq) \\ S(t \rightarrow \gamma q) &= 2 \times BR(t \rightarrow \gamma q) \times Br\,(W \rightarrow l\nu) \times \sigma(t\bar{t}) \times L \times \epsilon(t \rightarrow \gamma q) \end{aligned} \tag{8.16}$$

where $L = 10\,\mathrm{fb}^{-1}$, $\sigma(t\bar{t}) = 833$ pb, $BR(W \rightarrow l\nu) = 0.2136$, $BR(Z \rightarrow ll) = 0.0673$ ($l = e, \mu$), ϵ selection efficiency for the signal. From these formulae, the FCNC branching ratios $BR(t \rightarrow Zq)$ and $BR(t \rightarrow \gamma q)$ can be calculated for a given significance level S_{12}. Without the inclusion of systematic uncertainties, the sensitivity for a significance level of $S_{12} = 5$ is $BR(t \rightarrow Zq) = 11.4 \times 10^{-4}$ and $BR(t \rightarrow \gamma q) = 5.7 \times 10^{-4}$, also shown in Figure 8.17.

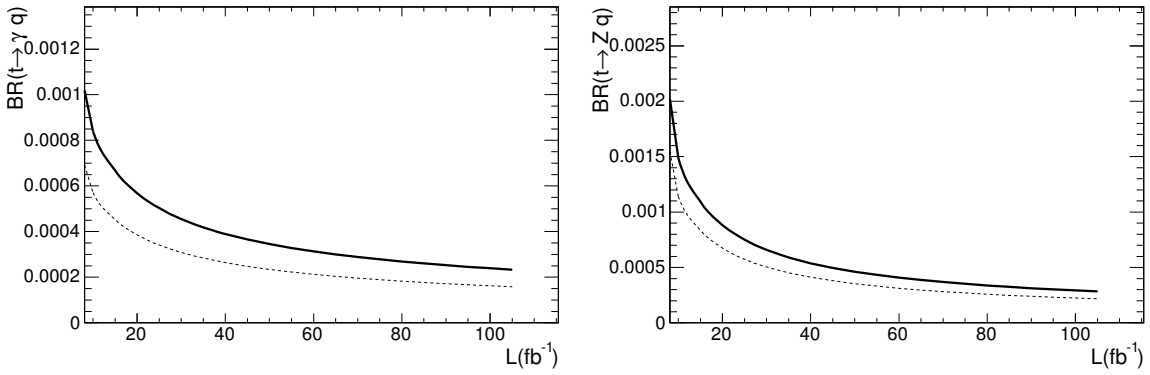

Figure 8.17: Branching Ratios of a FCNC signal detectable at the 5 sigma level as a function of the integrated luminosity, for the $q\gamma$ (left) and qZ (right) channels, shown with (solid line) and without (dashed line) systematic uncertainties.

The sources of systematic uncertainty are divided into two groups: those related to detector effects and those related to theoretical issues. For both kind of sources, the impact on the

selection efficiency and the surviving number of background events is evaluated. Experimental effects considered here include: (a) the lepton energy scale uncertainty, accounted for with relative increase/decrease of the reconstructed photon and electron four-momenta by ± 0.005; (b) the jet energy scale uncertainty, expected to lie in the range from $\pm 5\%$ at $p_{\mathrm{T}} = 20\,\mathrm{GeV/c}$ to $\pm 2.5\%$ at $p_{\mathrm{T}} > 50\,\mathrm{GeV/c}$, and totally correlated to missing energy uncertainty (assumed to be $\pm 5\%$, [319]); (c) b-tagging uncertainty (4% after $10\,\mathrm{fb}^{-1}$ integrated luminosity [284]), that is studied by assuming a non-b-tagged jet is actually a b-tagged jet 4% of the time; (d) uncertainty in anti-tagging b-jet instead of non-b ones (4% after $10\,\mathrm{fb}^{-1}$ integrated luminosity), simulated by assuming a b-tagged jet is a non-b-tagged jet with the same probability.

The impact of the single sources of systematic uncertainty is detailed in Table 8.28. Experimental sources of systematic uncertainties, such as the control of the lepton energy scale and of the b-tagging procedure are expected to be the most significant. The statistical uncertainty on the prediction of the background level of this analysis has a large contribution to the global systematic uncertainty. Refined techniques for the background estimation will reduce this uncertainty once data will be available.

Table 8.28: Effects of systematic uncertainties on the five-sigma observable FCNC branching ratios induced by different sources of systematic uncertainty. The last row indicates the smallest five-sigma observable FCNC branching ratios for $10\,\mathrm{fb}^{-1}$ of integrated luminosity including all sources of systematic uncertainty.

	$t \to Zq$ ($\times 10^{-4}$)	$t \to \gamma q$ ($\times 10^{-4}$)
$BR(stat)$	11.4	5.7
jet energy scale	+0.4	+0.6
b jet mistagging	+0.2	+1.8
light jet antitagging	+0.5	+0.9
lepton energy scale	+2.4	+0.5
$\sigma(t\bar{t})$	+0.1	+0.5
MC statistics in B	+2.4	+1.3
MC statistics in S	+0.7	+0.5
Luminosity	+0.1	+0.5
$BR(total)$	14.9	8.4

Including all systematic uncertainties, the smallest detectable FCNC branching ratios, for a five-sigma sensitivity and $10\,\mathrm{fb}^{-1}$ of luminosity, are $BR(t \to Zq) = 14.9 \times 10^{-4}$ and $BR(t \to \gamma q) = 8.4 \times 10^{-4}$. Under the assumption that the selection efficiency is unaffected by moderate instantaneous luminosity increases (i.e., pile-up), the decrease in the upper limit on the branching fraction with increasing luminosity can be evaluated in a straightforward way. Figure 8.17 shows the branching ratio for both channels as a function of the integrated luminosity. An improvement in the branching ratio limits by a factor of 2 is expected for a luminosity increase by a factor of 5.